LBL-17687

Lawrence Berkeley Laboratory

UNIVERSITY OF CALIFORNIA

RECEIVED
LAWRENCE
BERKELEY LABORATORY

DEC 19 1984

LIBRARY AND
DOCUMENTS SECTION

Materials & Molecular Research Division

ELECTROCHEMICAL PROCESSES AT THE SODIUM β'' ALUMINA INTERFACE

C.C. Mailhé
(M.S. Thesis)

May 1984

TWO-WEEK LOAN COPY

This is a Library Circulating Copy which may be borrowed for two weeks.

Prepared for the U.S. Department of Energy under Contract DE-AC03-76SF00098

LBL-17687

DISCLAIMER

This document was prepared as an account of work sponsored by the United States Government. While this document is believed to contain correct information, neither the United States Government nor any agency thereof, nor the Regents of the University of California, nor any of their employees, makes any warranty, express or implied, or assumes any legal responsibility for the accuracy, completeness, or usefulness of any information, apparatus, product, or process disclosed, or represents that its use would not infringe privately owned rights. Reference herein to any specific commercial product, process, or service by its trade name, trademark, manufacturer, or otherwise, does not necessarily constitute or imply its endorsement, recommendation, or favoring by the United States Government or any agency thereof, or the Regents of the University of California. The views and opinions of authors expressed herein do not necessarily state or reflect those of the United States Government or any agency thereof or the Regents of the University of California.

LBL-17687

Electrochemical Processes at the Sodium β" Alumina Interface

Catherine Colette Mailhé

University of California
Lawrence Berkeley Laboratory
Department of Materials Science
and Mineral Engineering
Berkeley, CA 94720

This work was supported by the Director, Office of Energy Research, Department of Materials Science Ceramics and Mineral Engineering of the U.S. Department of Energy under Contract No. DE-AC03-76SF00098.

TABLE OF CONTENTS

ABSTRACT v

TABLE OF FIGURES ix

INTRODUCTION 1

I. Structures 3

I.1 βAl_2O_3 3

I.1.1 Structure. 3

I.1.2 Non Stiochiometry. 3

I.1.3 Conduction Mechanism 6

I.2 $\beta''Al_2O_3$ 9

I.2.1 Structure. 9

I.2.2 Non Stoichiometry. 10

I.2.3 Conduction Mechanism 10

I.3 Relative Stability β/β'' 11

II. Modes of Degradation. 12

II.1 Mode I. 12

II.2 Mode II 13

III. Impurities. 15

III.1 Oxygen. 15

III.1.1 Na_2O 15

III.1.2 Chemical Coloration. 17

III.1.3 Water Uptake 18

III.2 Calcium and Potassium. 19

IV. Experimental Set up and Principle of the Measurement. . . 21

IV.1 Na/Na Cell. 21

IV.2 Principle of the Measurement/Use of a Reference Electrode. 24

IV.3 Four Point Measurement $\Delta I = f(E)$curves. 25

IV.4 I/E curves: Previous Studies. 27

V. Experimental Results and Discussion 30

V.1 Oxygen. 30

V.1.1 T = 350°C 31

A. Sodium 31

B. Na_2O 34

C. Vanadium 34

V.1.2 T = 160°C 38

A. Sodium 38

B. Na_2O 42

C. Vanadium 42

IV.1.3 Discussion Pile up/Depletion Model. 48

V.2 Water 53

V.2.1 Experimental Results 53

V.2.2 Discussion 54

V.3 Other Impurities Ca, K 54

V.3.1 Experimental Results 60

V.3.2 Discussion 61

VI. Conclusions 62

References. 63

Electrochemical Processes at the Sodium β" Alumina Interface

Catherine Colette Mailhe

University of California
Lawrence Berkeley Laboratory
Department of Materials Science
and Mineral Engineering
Berkeley, CA 94720

ABSTRACT

The influences of some impurities including oxygen, calcium and potassium on the polarization at the interface Na/β" alumina, were studied using a Na/Na cell. At 350°C, the normal operating temperature of the battery and at low current density (30-40 mA/cm^2) voltammetry indicated Ohmic interface behaviour. Deviations from this behaviour occurred only for higher current densities (100-150 mA/cm^2) and were accentuated at low temperature (160°C). Oxygen contamination caused an increase in resistance for sodium flowing in the β" alumina, this effect was explained by a pile-up at the interface of the oxygen present in the sodium and eventually formation of an oxide film, whereas the decrease in resistance associated with fresh sodium flowing out of the electrolyte could be attributed to a resultant decrease in oxygen concentration. The addition of vanadium to the sodium decreased the cell resistance. Vanadium is believed to reduce the oxide layer present at the surface of the β"Al_2O_3. Surprisingly, the addition of CaO, $CaCl_2$, Ca or KCl, which might have been expected to increase significantly the cell resistance did not result in such effects.

ACKNOWLEDGEMENTS

I wish to give my thanks here to all those who assisted me in the successful completion of this work.

To my advisor Professor L. De Jonghe for his constant guidance and helpful advice.

To Michel Armand for his fruitful ideas.

To Professor A. W. Searcy and Professor J. Evans who agreed to read this work.

To the competent technical staff for their constructive suggestions and contribution in the realization of my work.

To Diana Morris who typed this thesis.

And finally, to my research group whose friendship and help made this research work more enjoyable.

This work was supported by the Director, Office of Energy Research, Department of Materials Science Ceramics and Mineral Engineering of the U.S. Department of Energy under Contract No. DE-AC03-76SF00098.

Table of Figures

Fig. I.1 Sodium/Sulfur battery. 2

I.2 Structures of Na β and β"Al_2O_3 4

I.3 Conduction plane of βAl_2O_3 5

I.4 Conduction plane of β"Al_2O_3. 5

I.5 Roth defect. 7

I.6 β/β" phase diagram 8

III.1 Solubility of oxygen in liquid sodium. 16

IV.1 Na/Na cell 22

IV.2 Equivalent electrical circuit. 26

IV.3 Equivalent position of the (RE). 26

IV.4 Charge and discharge process 28

V.I-

V.13 Voltammetry curves 32

V.14 Oxygen concentration profile at the interface Na/β"Al_2O_3. 49

V.15 H_2O contamination voltammetry 55

V.16 β"Al_2O_3 tubes after cycling. 56

V.17 Cross section of β"Al_2O_3 tubes contaminated respectively by H_2O, CaO, $CaCl_2$ 57

V.18 KCl contamination voltammetry. 58

Table I. 59

INTRODUCTION

The Na/S battery has been the object of investigations and of great expectations for more than ten years because it constitutes a promising high energy density storage device for electric cars as well as for load leveling (Fig. I.1). This battery operates at 350°C so that the two reactants, sodium and sulfur, are in their molten state, separated by the $\beta''Al_2O_3$ solid electrolyte. The $\beta''Al_2O_3$ which prevents direct reaction of the two components, insures the transport of sodium ions which have been oxidized before they react with the sulfur to give a Na_xS_y sulfide. The main hindrance to the development of these batteries is the early failure of the $\beta''Al_2O_3$ tubes. The present work is concerned with the electrochemical aspects of the processes occurring at the interface between $\beta''Al_2O_3$ and Na. Severe polarization is deleterius for the efficiency and for the life time of the battery. Specifically, the work focusses on the influence of some impurities, namely oxygen, calcium, potassium, and examines the effects of water.

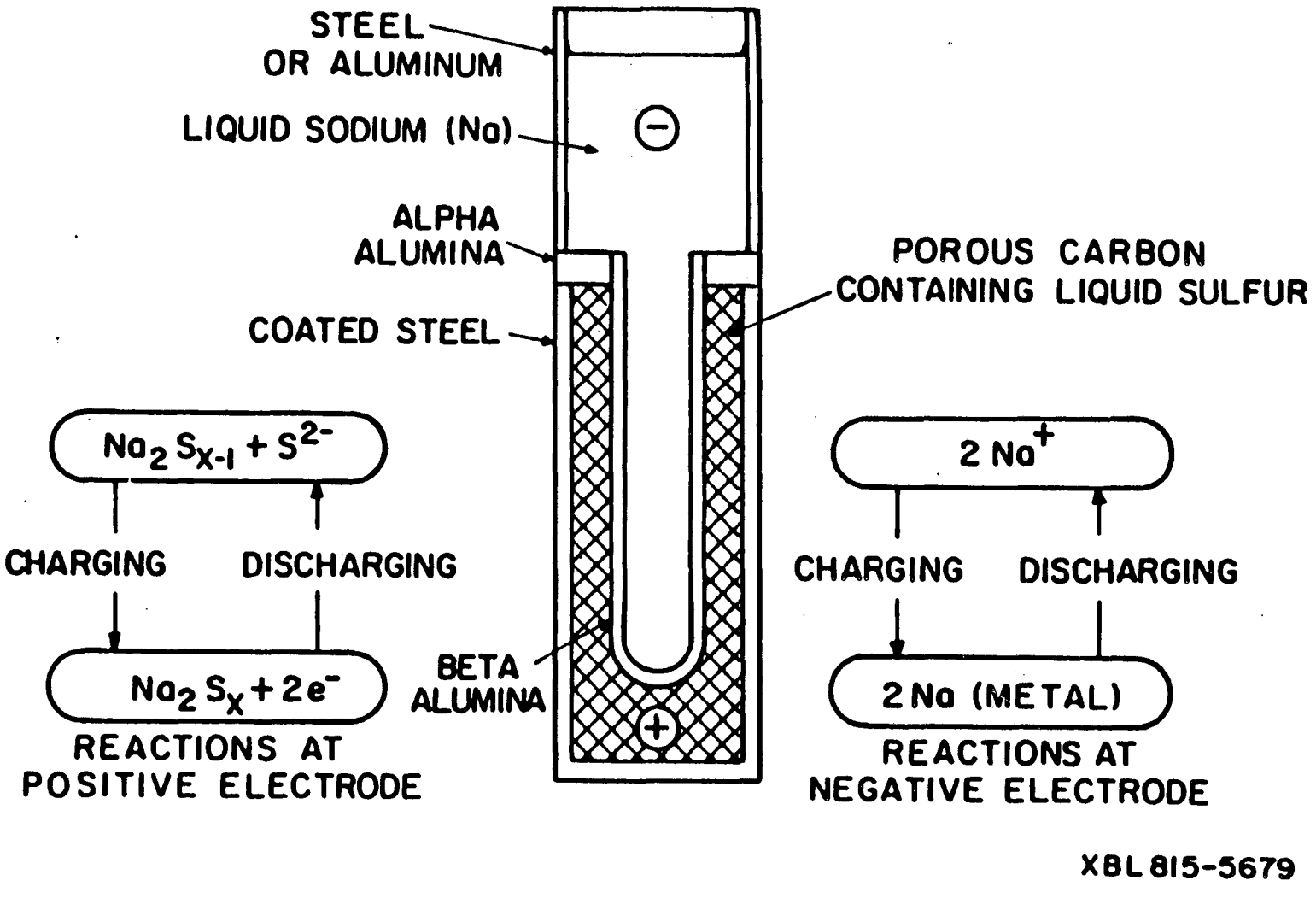

Fig. 1.1 Schematic cross section of the sodium/sulfur cell.

I. Structures of β and β"Al_2O_3 (Alumina)

β and β"Al_2O_3 are structurally closely related. In both cases Na^+ ions are "quasi" free to move in conduction planes separated by spinel-like blocks. Both materials exhibit high ionic conductivity. It is worth pointing out the structural differences between β and β"Al_2O_3 since these may account for their different electrochemical behavior.

I.1. βAl_2O_3

I.1.1 Structure (1). (Fig. I.2) Two "spinel" blocks (11Å) which are formed of planes of closely packed oxygens in which $Al3^+$ ions occupy octahedral and tetrahedral positions, separate the sodium conduction planes. Within the conduction planes Na^+ ions may occupy different positions: Beever-Ross (BR), anti Beever-Ross (aBR) and mid-oxygen positions (1). A BR position is constituted by the center of a triangular prism of six O^{2-}ions belonging to the oxygen planes from the spinel block above and below the conduction plane; an aBR position has two O^{2-}ions directly above and below (2.08Å spacing), and because of the associated strain is less energetically favorable.

I.1.2 Nonstoichiometry (2,3). The stoichiometric βAl_2O_3 is represented by the formula Na_2O ($11Al_2O_3$). In this case each Na^+ ion corresponds to one BR site (Fig. 1.3). In fact, there is a range of nonstoichiometries which correspond to an excess of Na^+ ions. The more general formula for the βAl_2O_3 can be written as:

$$c\ Na_2O\ \ (11Al_2O_3)$$

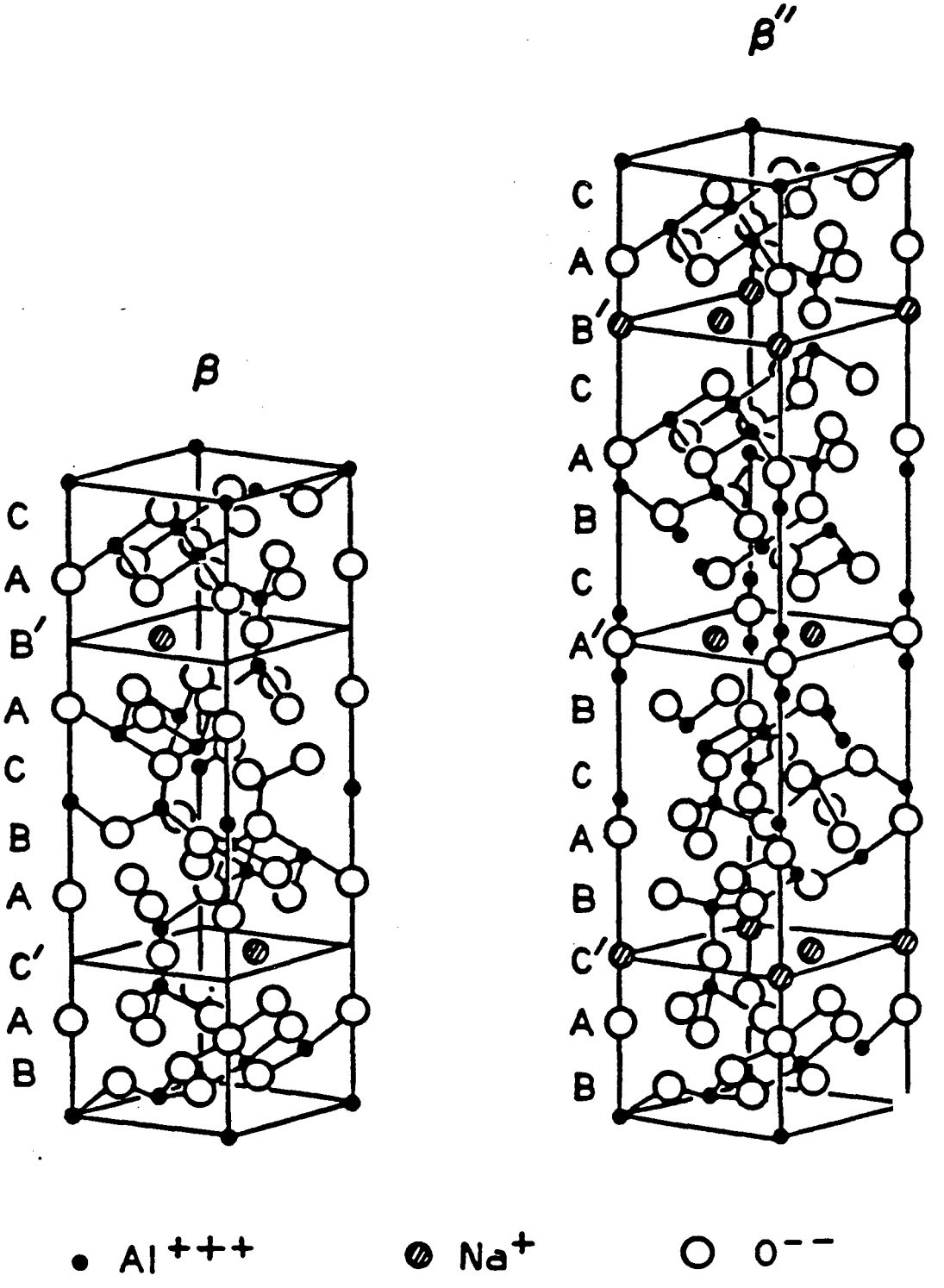

FigI.2 **Structures of sodium beta alumina and sodium beta" alumina.**

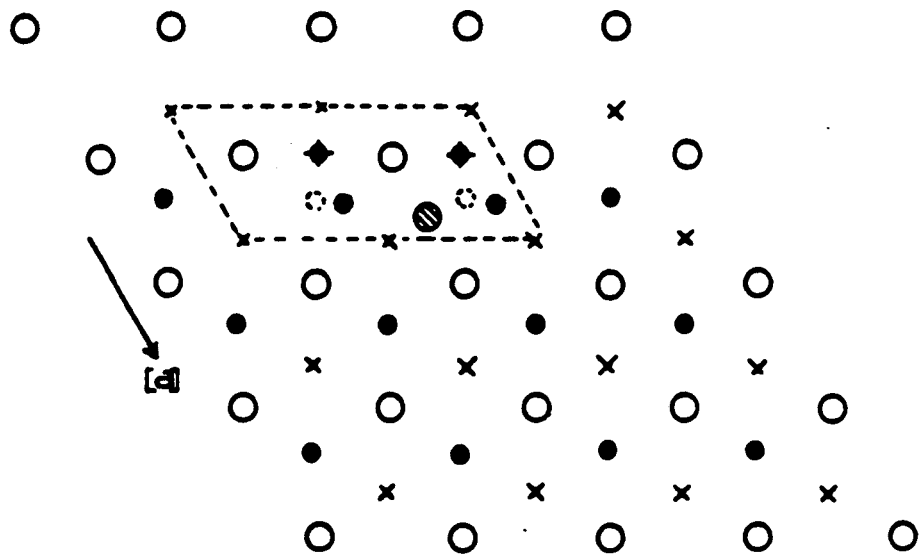

FIG13

○ OXYGEN
● SODIUM ON BEEVERS-ROSS SITE
⊘ OXYGEN INTERSTIAL
× ANTI BEEVERS-ROSS SITE (VACANT)
✦ SODIUM INTERSTIAL
◌ VACANT BEEVERS-ROSS SITE

XBL 8112-12951

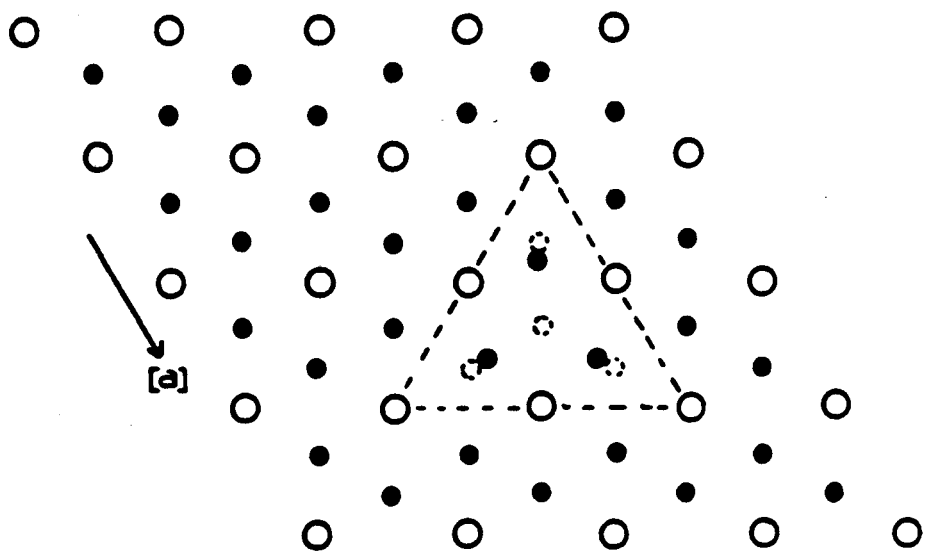

FIG14

○ OXYGEN
● SODIUM
◌ VACANT SODIUM SITE

Arrangement of ions in the conduction planes of: 13 sodium beta alumina; 14 sodium beta" alumina. Regions modified by point defects are enclosed by dashed lines.

with

$1.0 < c < 1.35$

The excess positive charge (2) has to be compensated: the first idea is to create Al^{3+} vacancies in the spinel block, especially as it has been shown that stoichiometric βAl_2O_3 exhibits departure from local electroneutrality according to the Pauling rule, i.e., the spinel block is too positively charged. Potential energy calculations show that the transfer of positive charge from the spinel block to the conduction plane is energetically difficult. The formation of Al^{3+} vacancies is thus unlikely, the replacement of Al^{3+} by divalent cations is a possibility, but the most satisfying compromise is reached with the Roth defect model (Fig. 1.5). The interstitial O^{2-}ion present at the mid-oxygen position in the conduction planes attracts the two neighboring Al^{3+} ions, displacing them to lead to the sequence V_{Al}-Al_i-O-Al_i-V_{Al} where V_{Al} represents an Al^{3+} vacancy and Al_i an aluminum interstitial. This defect, which can also be viewed as two Frenkel pairs and an additional Na_2O is not present in stoichiometric βAl_2O_3.

I.1.3 Conduction Mechanism (4-6). As already mentioned, the BR position represents a potential well for the Na^+ ion in stoichiometric βAl_2O_3 where almost all the BR positions are occupied. An excess of Na^+ ions tend to associate in pairs and occupy the mO position (Fig. I.3) (5). In a simplified model at 0 Kelvin for x excess cations, there should be 1-x ions on BR and 2 x on mO. Thus, the conduction involves

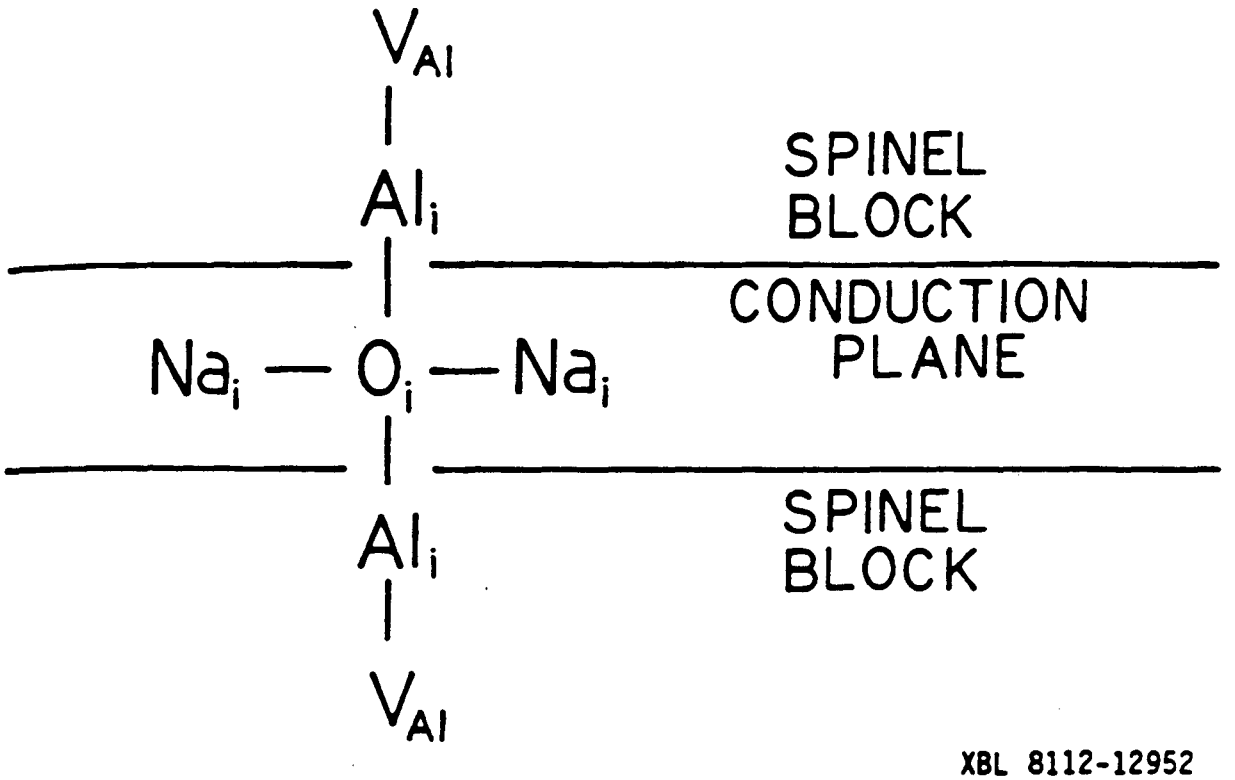

Fig. 1.5 Schematic representation of "Roth defect".

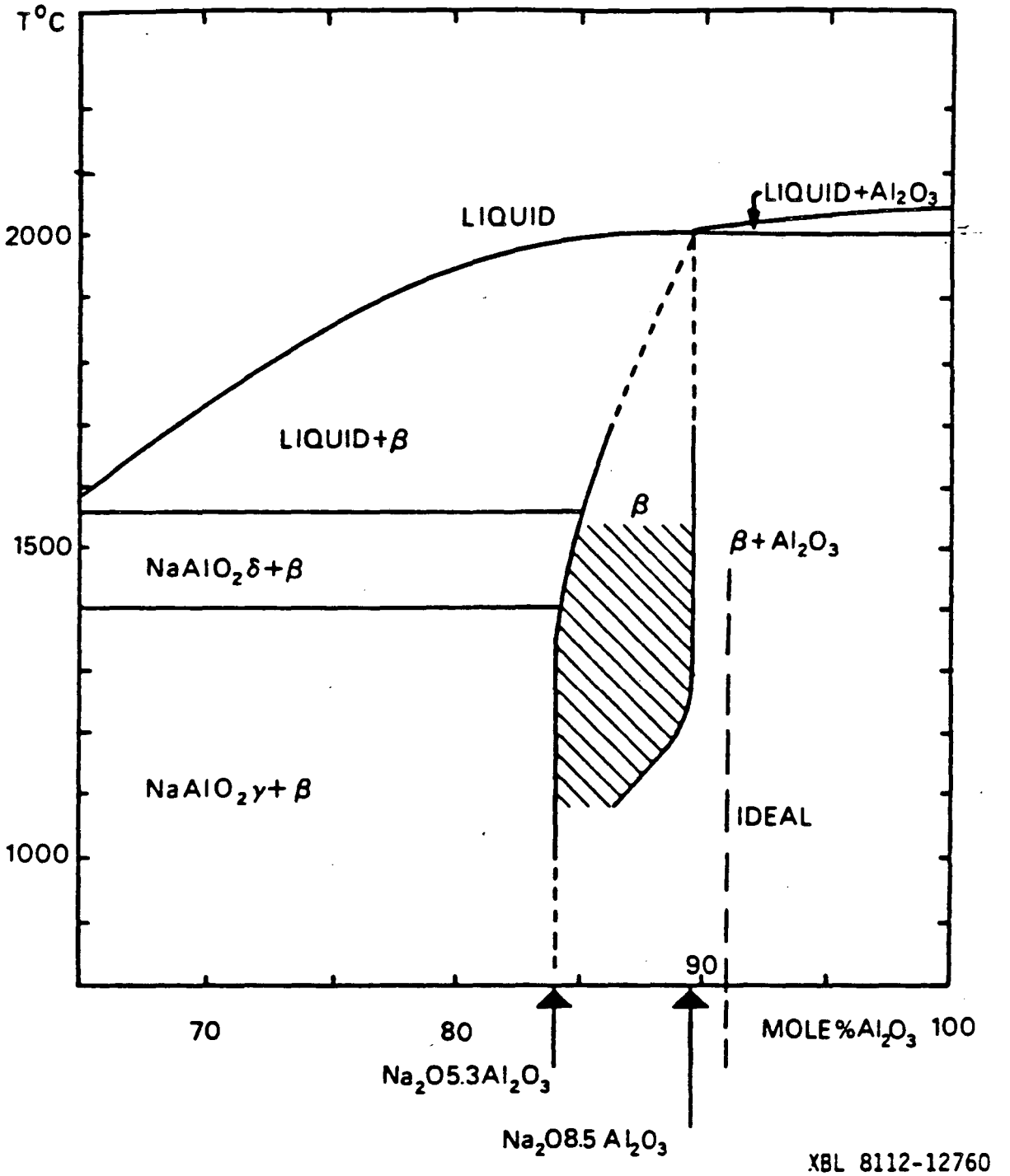

Fig.1.6 Proposed phase diagram of Na_2O-Al_2O_3 system in the region of existence of beta alumina phases. Shaded area represents region of coexistence of beta and beta" phases.

mainly pair motion; from an mO position the Na^+ cation may jump to a aBR configuration temporarily before occupying another mO position, leading to the sequence mO mO--->Br aBR--->mO mO. Due to the strong coulombic attraction between O^{2-} and Na^+ ions, the excess of Na^+ ions is confined to a region around the interstitial O^{2-}ions. This situation leads to the formation of big clusters of fixed O^{2-} (interstitial) surrounded by relatively free or mobile Na^+ ions. Thus, the nonstoichiometry of βAl_2O_3 is accommodated by these large clusters (6). Depending on temperature, Na^+ ions may escape from these regions and move from one region to another, producing ionic conduction through the whole conduction plane.

I.2 <u>$\beta''Al_2O_3$ (1)</u>

I.2.1 <u>Structure</u>. $\beta''Al_2O_3$ has almost the same spinel block/Na-conduction planes structure as βAl_2O_3 $\beta''Al_2O_3$ has a 3 spinel block sequence with a three-fold symmetry axis, whereas βAl_2O_3 has a 2 spinel block structure related by a two fold rotation. As a consequence the oxygen planes are always staggered with respect to each other and are not a mirror image of each other with respect to the conduction plane as they are in βAl_2O_3. In $\beta''Al_2O_3$ a Na^+ ion in the conduction plane occupies the center of a tetrahedron of four O^{2-}ions and there are two such positions per 1/3 unit cell. These two positions are energetically equivalent so that Na^+ does not move over aBR sites. In other words, the two distinct BR and aBR sites of βAl_2O_3 have been replaced by two equivalent sites. This explains immediately the higher ionic conductivity of $\beta''Al_2O_3$.

I.2.2 Nonstoichiometry. Stoichiometric $\beta''Al_2O_3$ is described by the formula Na_2O (5.33 Al_2O_3), but it also exhibits a range of nonstoichiometry in which about 17 percent of the conduction sites may be unoccupied (5), whereas βAl_2O_3 nonstoichiometry is characterized by an excess of Na^+ ions. Nevertheless, $\beta''Al_2O_3$ is much richer in Na content than βAl_2O_3.

Very often MgO and LiO (7,8) are used to stabilize the β" phase. Mg^{2+} or Li^+ can replace Al^{3+} in the spinel block to maintain charge balance. Thus, no compensating O^{2-}ions (equivalent to the mid O of βAl_2O_3) are found in the conduction plane.

I.2.3 $\beta''Al_2O_3$ Conduction Mechanism (5,9). The conduction mechanism is expected to be insured by vacancies (Fig. 1.4). The activation energy for the motion of a vacancy is very low, 0.02 eV (5). The ionic resistivity of polycrystalline $\beta''Al_2O_3$ at 350°C is 3-4 Ωcm (compared to 15-20 for βAl_2O_3). The vacancies interact easily due to their high mobility, and as a result may get ordered in clusters or microdomains, especially when divalent impurities are present (9). The temperature has an influence on the domain coherence length, an increase in temperature leading to a rapid decrease in the latter. The decrease in the coherence lengtn leads to a decrease in the activation energy, E_a. E_a is therefore very much temperature dependent and this may explain the observed non-Arrhenius behavior of the Na^+ion diffusion in $\beta''Al_2O_3$. A comparison has been drawn between $\beta''Al_2O_3$ and Na rich βAl_2O_3 of the same composition stabilized by Mg. A 2 dimensional long range order is present in

βAl_2O_3 whereas a limited coherence length is found in β". There are many more sites available for conduction in $\beta''Al_2O_3$ since the previous BR and aBR sites of βAl_2O_3 have become equivalent in $\beta''Al_2O_3$ (the disorder is thus much more extensive).

As a conclusion, conduction in βAlO_3 involves motions of Na^+ pairs from (mO–mO) sites to (BR–aBR) sites, whereas in $\beta''Al_2O_3$ it involves motions of vacancies. Short range order and formation of clusters occur in both cases, but since in $\beta''Al_2O_3$ the Na^+ sites corresponding to BR and aBR sites have become equivalent, the disorder is more important.

I.3 Relative Stability β/β" Phase Diagram (10) (Fig. 1.6)

The binary system Al_2O_3/Na_2O has been studied extensively for years but the range of stability or metastability of β" with respect to β is still a matter of investigation. Annealing experiments at 1400°C and 1500°C of the eutectic composition show an increase in the proportion of β with respect to β" with increasing annealing time proving that β" is thermodynamically metastable in the binary system Al_2O_3/Na_2O. But the kinetics of transformation are very slow. The mechanism of transformation β"⟶β is still not established unambiguously as the proportion of β" increases with decreasing cooling rate, which doesn't agree with a classical nucleation and growth mechanism.

II. MODES OF DEGRADATION

Failure of the $\beta''Al_2O_3$ tube signifies a short circuit and the end of the battery since a crack, which has propagated all the way through the electrolyte, allows the sodium and sulfur to react directly. The modes of degradation of $\beta''Al_2O_3$ under electrolytic conditions, i.e. when sodium is actually flowing through the electrolyte are briefly reviewed here and the possible influence of impurities is indicated. Two modes of degradation have been evidenced: mode I and mode II (11).

II.1 Mode I

In Mode 1 degradation a preexisting flaw at the surface of the electrolyte propagates under the Poiseuille pressure which develops inside the crack where sodium ions are reduced. According to fluid mechanics, the liquid sodium, like any fluid being forced out of a capillary channel, develops a pressure inside the crack leading to further opening of the flaw. Thus, the mode I degradation occurs during the charging cycle of the battery, so that cracks are only initiated on the sodium exit side of the $\beta''Al_2O_3$ tube. This model was first proposed by Armstrong (13). Tennenhouse (14) suggested a dissolution mechanism of the electrolyte at the crack tip. Accoustic emission studies evidenced a critical current density for the onset of crack propagation (15).

Mode I crack propagation is mainly a mechanical effect-a Poiseuille pressure-therefore refined fracture mechanics with different crack geometry was used in the attempt to relate the critical current

density for failure to the stress intensity factor, K_{IC}, of $\beta''Al_2O_3$. The critical current density for failure was always found to be several orders of magnitude lower than the density predicted from fracture mechanics and measured K_{IC}.

However, current enhancement may occur around non-wetted or poorly conducting areas. In this respect impurities may play a role: segregation of impurities would lead to poorly conducting area around which current density enhancement might occur, these impurity enriched regions would constitute preferred sites for the initiation of cracks.

Mode I degradation even with current or enhancement effects cannot account solely for the breakdown of the tube, the current density threshold for failure being much lower than the one predicted by this model.

II.2 Mode II

Mode II degradation is associated with a different process which consists of the internal deposition of Na metal under pressure inside the electrolyte and subsequent microcracking originating from these regions. The proposed explanation for this internal electrolysis (Na ions being reduced to metal) is the following: $\beta''Al_2O_3$ may undergo some reduction when in prolonged contact with sodium. The solid electrolyte accepts oxygen vacancies, the additional charge being compensated by electrons. This incorporation of electrons leads to a gradient in electronic conductivity through the material. The expression for the electrochemical potential of sodium under electrolytic conditions which has been derived by De Jonghe, and

appears to be composed of two terms (17). A first term represents the open circuit conditions; a second term is the product of the applied voltage and a function of the gradient of the electronic conductivity.

For sufficiently high applied voltages, the electrochemical potential of sodium can take positive values with respect to the metal electrode, which means that sodium metal can be formed under pressure inside the electrolyte.

The British Rail work (unpublished) has established some correlations between the presence of Ca and some cracks associated with a mode II type of degradation. In the present study, we are more concerned with the electrochemical process at the interface and the modifications brought by impurities, in the normal range of operation of the battery where these modes of degradation should not occur, at least not at the beginning of the cell operation. However, for both modes the presence of impurities lowers the critical current density, leading therefore to premature failure of the tube.

III. IMPURITIES

The range of impurities that may have an effect on the electrochemistry of the system $\beta''Al_2O_3/Na$ is wide. A choice has to be made. The oxygen seems to be among the first ones to focus on as it may be involved in different forms, e.g. in Na_2O and H_2O, and in different processes such as formation of an oxide Na_2O layer, water-uptake by the electrolyte, and electrolytic reduction.

Calcium and potassium will also be considered since they are known to be deleterious to the life time of a battery (36,37). This list is far from being exhaustive. This study is also limited to the influence of impurities present in the liquid sodium, neither the importance of impurities on the sulfur side (because apparently the sulphur side is less troublesome than the sodium side) (23), nor the effects due to the doping of the $\beta''Al_2O_3$, prior to sintering or during postsintering, have been taken into account. Along this line, a recent paper has shown that a postsintering treatment of $\beta''Al_2O_3$ with selenium could decrease significantly and favorably the resistivity and increase the life of the battery (18).

III.1 Oxygen

III.1.1 <u>Sodium Oxide Na_2O</u>. According to the binary phase diagram Na/O, the solubility of oxygen in sodium is about 250 ppm by weight at 350°C (Fig. III.1). The presence of Na_2O (19) is thus very likely in the sodium electrode of a sodium/sulfur battery and may result in the local formation of a resistive layer at the sodium/solid electrolyte interface. Na_2O formation will cause inhomogeneities in

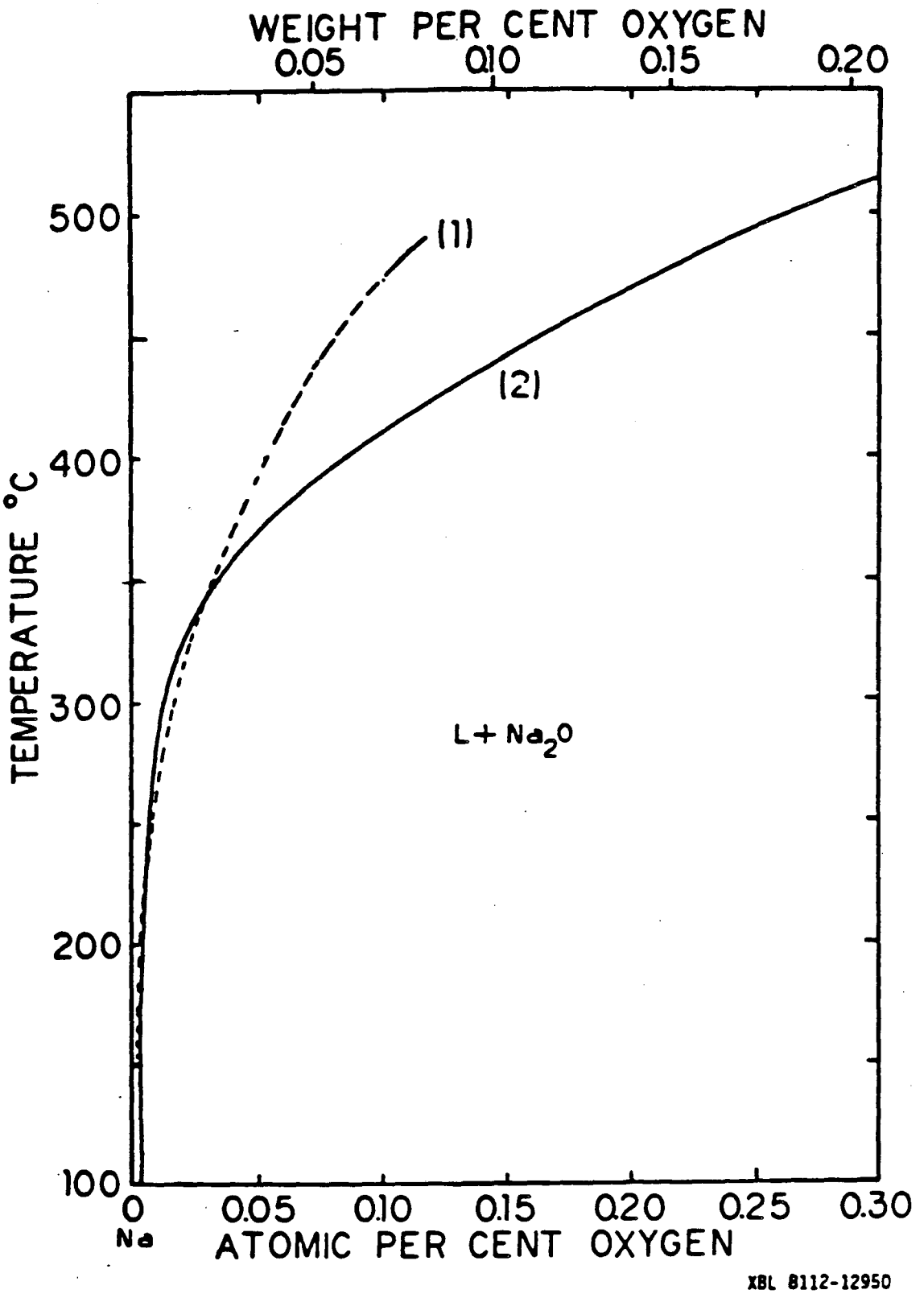

Fig III.1 **Solubility of oxygen in liquid sodium.**

the current density distribution which may locally exceed the critical current density for failure. An oxide layer could also contribute to a poor wetting of $\beta''Al_2O_3$ by the molten sodium. A good wetting is necessary to insure a low charge transfer resistance and therefore a long lifetime. Contact angle studies (19-21) have shown that good wetting is achieved only at temperature higher than 300°C (optimum at 370°C). Along the same line, current density enhancement will occur around nonwetted or poorly wetted area. An additive that could improve the wetting behavior would be highly useful.

III.1.2 Chemical Coloration of $\beta''Al_2O_3$ (22-23). $\beta''Al_2O_3$ undergoes a darkening when immersed in molten sodium. This discoloration effect has been attributed to the reduction of $\beta''Al_2O_3$ by sodium which can be written as

$$O^{2-} \longrightarrow 1/2O_2 + 2e^-.$$

The reaction produces an oxygen vacancy in the β or $\beta''Al_2O_3$. Oxygen vacancies compensated by electrons are created at the surface of the electrolyte and can diffuse through the spinel block. The simultaneous injection of electrons leads to an electron/ion transport number gradient which is at the origin of the mode II of degradation, formation of clusters of metallic sodium inside the material. This discoloration phenomenon is reversible; when the electrolyte is exposed to oxidizing conditions, bleaching occurs mainly through the conduction planes. Water seems to have very little effect (23). In

the present case of polycrystalline materials, grain boundaries are a preferential path for diffusion of these defects.

III.1.3 Water Uptake by $\beta''Al_2O_3$ (24,25). $\beta''Al_2O_3$ is well known to be more sensitive to moisture than βAl_2O_3 (25). Water seriously affects its electrical and mechanical properties, which represents an hindrance from a technological point of view in the handling of an Na/S battery if the required precautions are not taken. Therefore, it is certainly worth investigating the extent of the damage caused by water.

H_2O molecules or hydronium ions H_3O^+ may enter the conduction planes and an ionic exchange takes place with the mobile conducting Na^+ ions of the conduction plane (24). Thermogravimetric (26) analysis and differential thermal analysis makes it possible to differentiate two sites for water incorporation, surface adsorption, and a bulk intercalation. Microbalance experiments show a rapid water uptake, certainly associated with a surface phenomenon, followed by a slower rate for the bulk hydration. The existence of a hydrated surface layer has been evidenced by x-ray diffraction (27). β'' (and β) undergo a lattice expansion caused by the intercalation of water and c_0 (lattice parameter) reaches asymptotically the value obtained for $H_3O^+\beta''Al_2O_3$ (H_3O^+ exchanged, β'' alumina) H_2O can also move rapidly along the grain boundaries.

Carbonate species Na_2CO_3, $NaHCO_3$ (28) have been found at the surface of the electrolyte. Most probably when H_2O enters the

structure, Na^+ comes out to give hydrated Na_2O, which is an efficient getter of CO_2.

The increasing sensitivity (26) to moisture of various $\beta''Al_2O_3$ isomorphs, Ag, Na, Li $\beta''Al_2O_3$, may be explained in terms of interactions cations—H_2O dipoles: Li$\beta''Al_2O_3$ is more sensitive than the other isormorphs, but Li^+ ion is also the most polarizing ion of the three Ag^+, Na^+, Li^+. The sensitivity of the electrolyte depends also on the stabilizing agents such as Mg and Li which are incorporated in the spinel blocks (25).

With respect to the electrical properties of $\beta''Al_2O_3$, the water is expected to cause an increase in the resistance. A study (29) with the system $CPNaAsF_6/\beta''Al_2O_3/CPNaAsF_6$ (CP: propylene carbonate) at room temperature showed an increase in the resistivity and a non-Ohmic behavior within a few days for β'' exposed to moisture. The radial resistance of the tube increased more than the longitudinal resistance which supports the idea that the hydration is first of all a surface phenomenon.

Fortunately the water intercalation is reversible and $\beta''Al_2O_3$ properties may be restored by heating at $T > 600°C$. In the case of Na/S battery, which operates at 350°C, there would be still a residual resistance.

III.2 Influence of Calcium and Potassium

The βAl_2O_3 family exhibits interesting ionic exchange properties. A wide range of ions can enter the structure and replace the Na^+ ions. In some cases a complete ionic exchange (30-35) is

achieved by immersion of $\beta''Al_2O_3$ in a molten salt. Numerous papers have been published recently about divalent cation βAl_2O_3 (Ba^{2+}, Ca^{2+} ...).

Due to its open structure $\beta''Al_2O_3$ may intercalate very easily many kinds of impurities, (34), but only some species exhibit high diffusion coefficients, although always lower than the one of sodium. Therefore, impurities will impede the transport of sodium, leading to an increase in the resistance.

In our study, the material is polycrystalline, grain boundaries may act as preferential paths for diffusion. Experiments have been conducted in a $Na/\beta''/Na_2S$ cell, impurities being added on the sulfur/polysulfide side. It has been shown that Ca^{2+} ion is the most deleterious impurity and concentrates at grain boundaries leading to a tremendous increase in the resistivity (36-37) (increase of 10-20 times in 50 hours of cycling for a current density of 25-30 mA). Some cracks were eventually observed. Potassium contamination leads to a 2 to 3 fold increase in resistivity, and its distribution becomes more homogeneous as current is passed. On the other hand, when Ca^{2+} exchange was conducted on a single crystal of $\beta''Al_2O_3$, the conductivity first increased for small amounts of Ca^{2+}-ion exchanged, and then decreased sharply (33). The initial increase has been attributed to the creation of vacancies ($2Na^+$ ions are replaced by one Ca^{2+} ion), but as the concentration of Ca^{2+} ions increases, the interaction Ca^{2+}-vacancy is stronger and leads to formation of ordered defect groups, therefore the mobility of vacancies is strongly decreased.

IV. EXPERIMENTAL SET UP AND PRINCIPLE OF THE MEASUREMENT

IV.1 Na/Na Cell (Fig. IV.1)

A Na/Na cell was designed along the same lines as the one used by Breiter and Dunn (38,39). The choice was made at the beginning to operate the cell outside the glove box. Therefore the main constraints were to maintain the cell argon tight and sodium corrosion resistant at 350°C.

The body of the cell is made of stainless steel, which exhibits a reasonable resistance to sodium corrosion. Aluminum has a better sodium corrosion resistance but the welding of any feedthroughs would have been troublesome.

This cell is a classical three-electrode electrochemical setup with a working, a reference, and a counter electrode (38). The working electrode (WE) is a rod of nickel. A nickel wire is attached at the end and wound in a spring like fashion to insure an electrical contact with the $\beta''Al_2O_3$ tube at the beginning of the electrolysis. This spring may produce some notches on the inside surface of the tube when assembling the cell. A graphite cloth would have been better in this respect but also would have introduced some unknown impurities.

The reference electrode (RE) is a thin nickel wire passing through a boron nitride lid and sticking out of the groove of the lower part of the lid in such a way that the contact with the top of the tube is insured. The wire is chosen to be flexible enough to let the boron nitride lid dangle outside the upper part of the cell and,

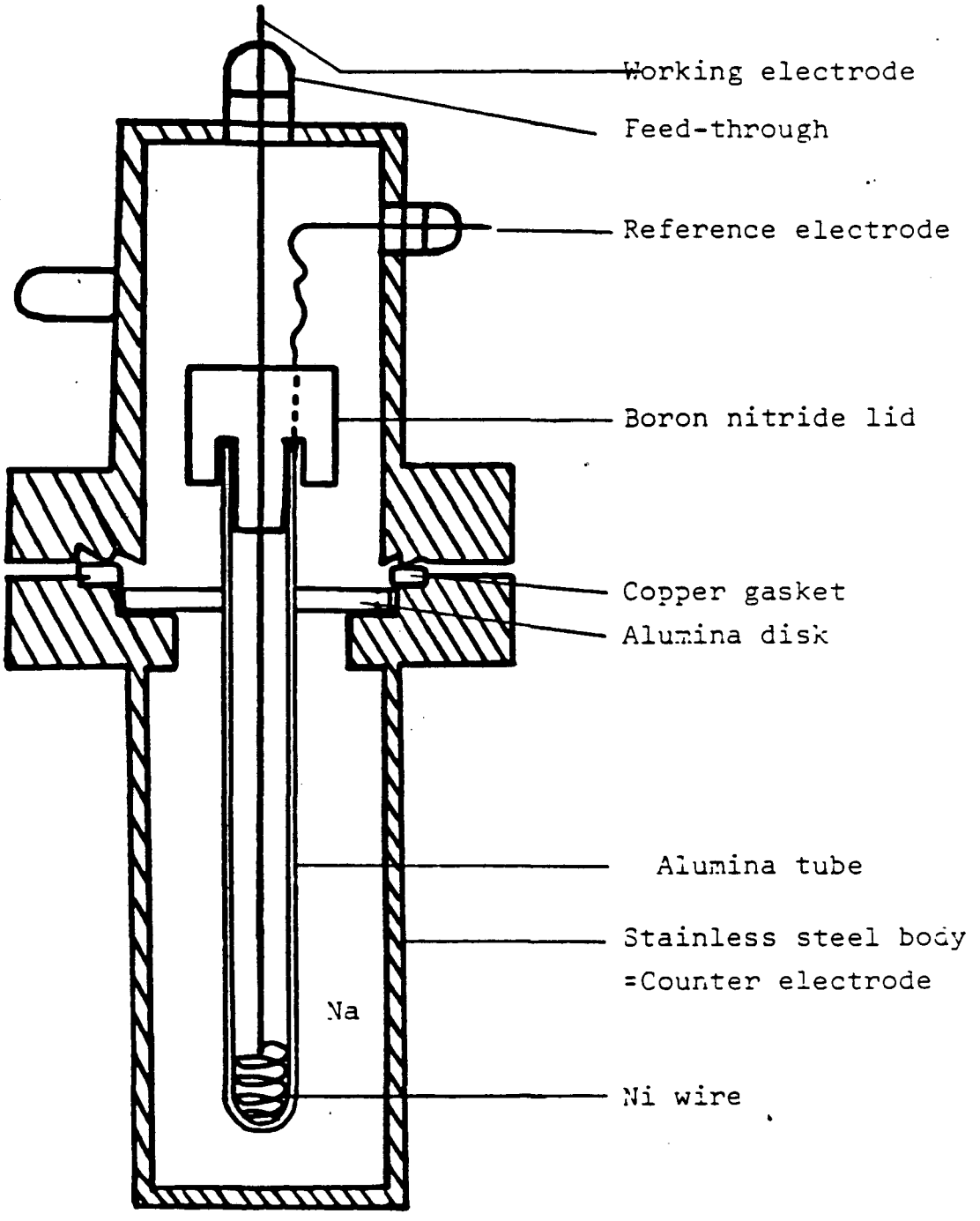

Fig.IV.1 **Na/Na cell**

when the cell is assembled, is adjusted on the top of the tube and slides back in position along the nickel rod when closing the cell.

The counter electrode (CE) is the stainless steel body of the cell. The $\beta''Al_2O_3$ tube is attached to an αAl_2O_3 disk by a glass seal.

The electrical connections for the (RE) and (WE) are provided by a feedthrough of glass/kovar type (to insulate them from the main body of the (CE)). These feedthroughs are also vacuum tight. Ordinary feedthroughs could not be used as they were not sodium corrosion resistant.

The cell is assembled in the glove box. The sodium used is saturated with oxygen and contains some sodium oxide. Some sodium is melted in the lower part of the cell and will constitute the (CE). The $\beta''Al_2O_3$ tube is then dipped slowly in the molten sodium and the αAl_2O_3-disk is adjusted at the top of this half cell. The (WE) slides inside the $\beta''Al_2O_3$ tube and the boron nitride lid is adjusted at the top of the tube to insure a contact for the (RE). After the nuts have been tighten, the cell is taken outside the glove box and all experiments can be carried out in a furnace with an air atmosphere. The temperatures of the experiments range between 160 and 350°C.

The $\beta''Al_2O_3$ is filled electrolytically--usually 1.5 cm^3 of sodium are electrolysed inside. Some current is also drawn at the tip of the (RE) in order to build a minute droplet of Na which constituted the (RE). The cells were also dismantled in the glove box.

IV.2 Principle of the Measurements--Use of a Reference Electrode

Current versus voltage curves can characterize the electrode/ Electrolyte interface --in our case molten Na/β"Al_2O_3. Deviations from Ohmic behavior indicates that one or several steps of the interface process(es) are kinetically limited, for example diffusion limitation of the electroactive species transported from the bulk to the interface. This gives rise to overvoltages or so-called polarization (42).

In all electrochemical measurements a difference of potential is imposed (respectively measured) in beween the (RE) and the (WE) and the corresponding current flowing between the (WE) and the (CE) is measured (respectively, imposed). This need for three electrodes comes from the fact that only a difference of potential can be measured and therefore a constant stable potential is necessary as a "reference potential". The potential of the (CE) is not suitable for a reference since current is flowing through it and an overvoltage may be generated if the (CE) interface is non-Ohmic. The (RE) is in our case the droplet of Na at the top of the tube. That (RE) is connected to an electrometer of high impedance so that very little current is actually flowing in between the (WE) and the (RE).

An electrical circuit equivalent to the electrochemical cell can be drawn (Fig. V.2). Only resistors have been considered. This is of course an oversimplification. Interfaces are better modeled by impedences, but this simple description helps nevertheless in the understanding of the role of the (RE).

The main purpose of this (RE) is to differentiate the two $Na/\beta''Al_2O_3$ interfaces inside and outside the tube. As the potential of the (WE) is monitored with respect to a (RE) and the potential of this (WE) is directly dependent on the sodium activity, we have here a direct insight on the interface processes.

The resistance which appears on the graph I/E is composed of the (WE) interface resistance $Na/\beta''Al_2O_3$ and part of the bulk resistance of the electrolyte. This resistance is schematically represented in Fig. IV.3.

If the inside of the tube is then contaminated with one specific impurity, its effect on the interface process is investigated without any interference with what is occurring on the other side, and any non-Ohmic behavior may then be related to this specific impurity.

IV.3 Four Point Measurement $\Delta I = f(E)$ Curves

A substantial improvement in the sensitivity of the method was obtained with a four probe measurement: two probes to measure the potential and two probes (two current leads) to carry and measure the current. The additional potential probe is a nickel wire welded onto the (WE). As a matter of fact, it appears that the electrical connections inside the furnace were subjected to oxidation, therefore residual resistances were introduced. The introduction of a separate probe to measure the potential eliminates the difficulty.

As it will be seen in the following, the deviations from a purely Ohmic behavior are slight, therefore a way of accentuating the non-Ohmic effects is to plot $\Delta I = f(E)$ where $\Delta I = I - I_{ohmic}$ and

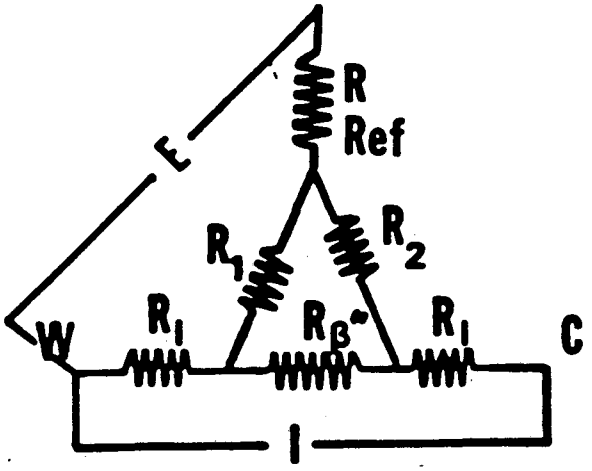

R_I=R interface Na/ Al_2O_3

R=resistance of β″ tube(1 mm thick).

I=current

E=potential

R=Electrometer resistance

W:working electrode

C=counter electrode

Ref.=reference electrode.

R_1 and R_2 are much higher than R as the (RE) is positioned at the top of the tube.

Fig.IV.2 Equivalent electrical circuit.

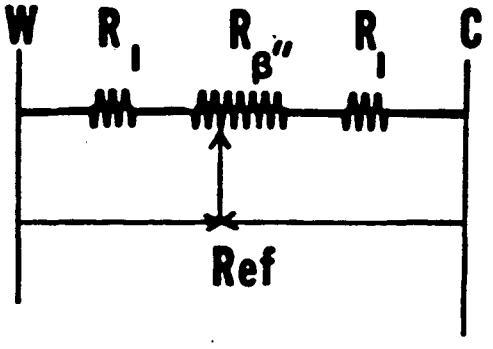

Fig.IV.3 Equivalent position of the (RE).
Same symbols as in Fig.IV.2.

I_{ohmic} represents the hypothetical, purely Ohmic behavior. This is equivalent the main Ohmic contribution.

IV.4. Curves I/E Previous Studies (38-41)

An ideal interface electrode electrolyte exhibits an Ohmic behavior. Deviations from the ohmic behavior and polarization which may occur are deleterious to the capacity storage and the life time of a battery. Resistance rise and asymmetry with respect to the direction of the current flow were observed in β and β" electrolytes. Usually the ratio $R_{discharge}/R_{charge}$ is bigger than 1 (during discharge, $Na \longrightarrow Na^+ + e^-$, metallic Na enters the electrolyte, during charge, $Na^+ + e^- \longrightarrow Na$, Na flows out of the electrolyte (Fig. IV.4).

The relative percentage of β and β" has a drastic influence on the electrochemical behavior of these electrolytes (38). Pure β"Al_2O_3 displayed an ohmic behavior whereas the mixed composition with 70 percent β" exhibited an asymmetry $R_d/R_c > 1$ with no time dependance and the 80 percent β" composition exhibited an asymmetric behavior with time dependence. In the last case the I/E-curves exhibited electrochemical waves as if the electroactive species present in a film at the surface were oxidized or reduced and were therefore contributing to the anode or cathode current. The waveshape of these curves may be explained in terms of kinetic and diffusion limitations as in any voltammetry performed on thin films. When the potential reaches the value E°, at which the electroactive species may be reduced or oxidized, the reaction occurs giving rise to a current density, I, which increases up to the point where diffusion limitation

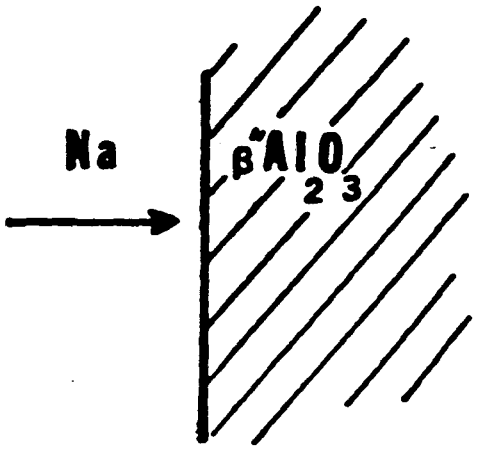

DISCHARGE

$Na \rightarrow Na^{+} + e^{-}$

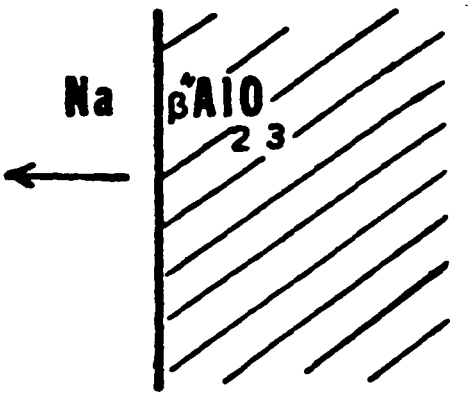

CHARGE

$Na^{+} + e^{-} \rightarrow Na$

FIG IV 4

or depletion of the reacting species occurs, causing it to decrease. This explains the wave shape of these curves. The film at the surface was believed to be a mixture of Na/Na_2O and apparently the presence of this film was evidenced only for certain compositions of the mixture $\beta/\beta''Al_2O_3$. One question is whether the structural differences in between β and $\beta''Al_2O_3$ can really account for such drastic differences in the electrochemical behavior.

The electrolyte studied in the present research is nearly pure $\beta''Al_2O_3$ for which an Ohmic behavior has been reported (38). It is nevertheless important to investigate now to which extent impurities could be responsible for deviations from Ohmicity.

V. EXPERIMENTAL RESULTS

V.1 Oxygen

The following results have been obtained with a four probe electrochemical cell. Regarding the experimental conditions, two points have to be determined, the range of current density and the temperature under which the tubes have to be tested.

Acoustic emission studies have evidenced a lower critical current density for the initiation of failure of about 150 mA/cm^2. The 30-50 mA/cm^2 current density region seems to be a reasonable range to explore first as the phenomena that may occur then could be attributed uniquely to the effect of impurities, oxygen in this case, without interaction with a possible crack propagation. Nevertheless tubes were tested up to 100-150 mA/cm^2 in order to observe interesting deviations from the ohmic behavior.

The normal operating temperature of the battery is 350°C. However, experiments were conducted at a lower temperature (160°C) since lower temperature experiments provide more information regarding the kinetic process.

One way of determining the role of the oxygen is to vary and control its activity in the sodium. The amount of oxygen present in the tube is controlled either by adding sodium oxide Na_2O--the activity of the oxygen is then fixed by the solubility product Na/Na_2O--or by adding some vanadium foil. Vanadium reduces Na_2O (cf. Ellingham diagram), and fixes the oxygen activity in the sodium

electrode at a lower value. Cells containing only the electrolyzed Na were also tested for comparison. As a summary, three different types of cells were tested "pure" Na, and Na + Na_2O, Na + Vanadium foil, at 350°C and at 160°C.

V.1.1 Normal Operating Temperature T = 350°C.

A. Pure Sodium. sodium is electrolysed inside the β"Al_2O_3 tube. More realistically the main potential contaminant is certainly the oxygen. The possible sources of oxygen contamination are the following: H_2O molecules adsorbed on the surface of the β"Al_2O_3 tube, O_2 from the argon atmosphere of the glove box and Na_2O contained in the sodium of the counter electrode. This contribution is certainly negligible compared to the two others because the oxygen partial pressure is very low and therefore the transport of oxygen from the outside to the inside of the tube through the gas phase is negligible.

Curves I/E current/Potential (Fig. V.1, V.2). In the low current density range (30/40 mA) the behavior is strictly Ohmic, for higher current density only two tubes have been tested and will be called α and β in the following. At high scan rates (100 mV-20 mV/s) the behavior is Ohmic. Some deviations from this Ohmic behavior and hysteresis occur at slower scan rate (1 mV/s), especially in the case of cell β. These deviations correspond to a decrease in the resistance for fresh sodium flowing in the tube and to an increase in the resistance for sodium flowing out. The range of resistance changes is between 0.06Ω and 0.09Ω. It is interesting to point out

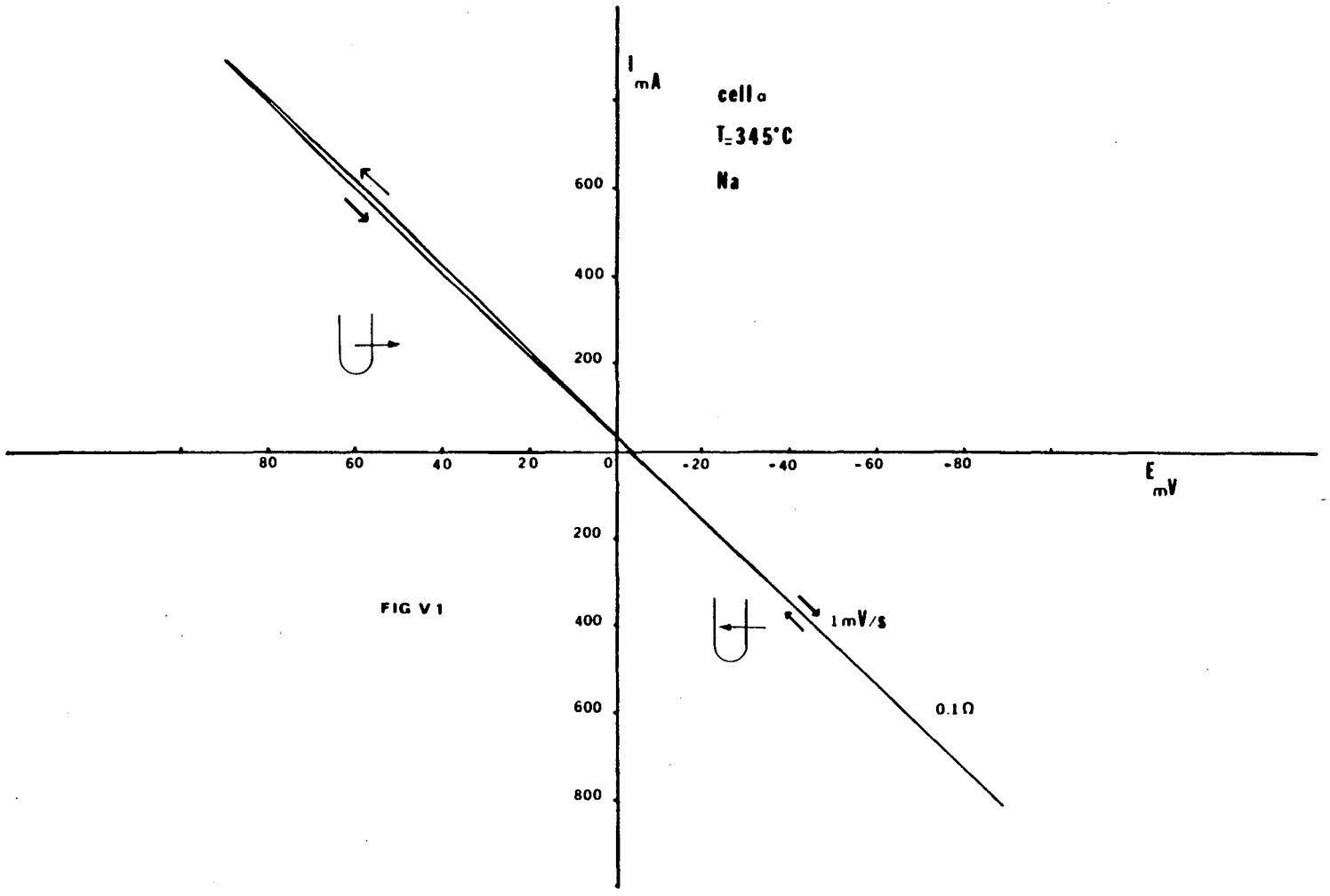

FIG V 1

XBL 845-1676

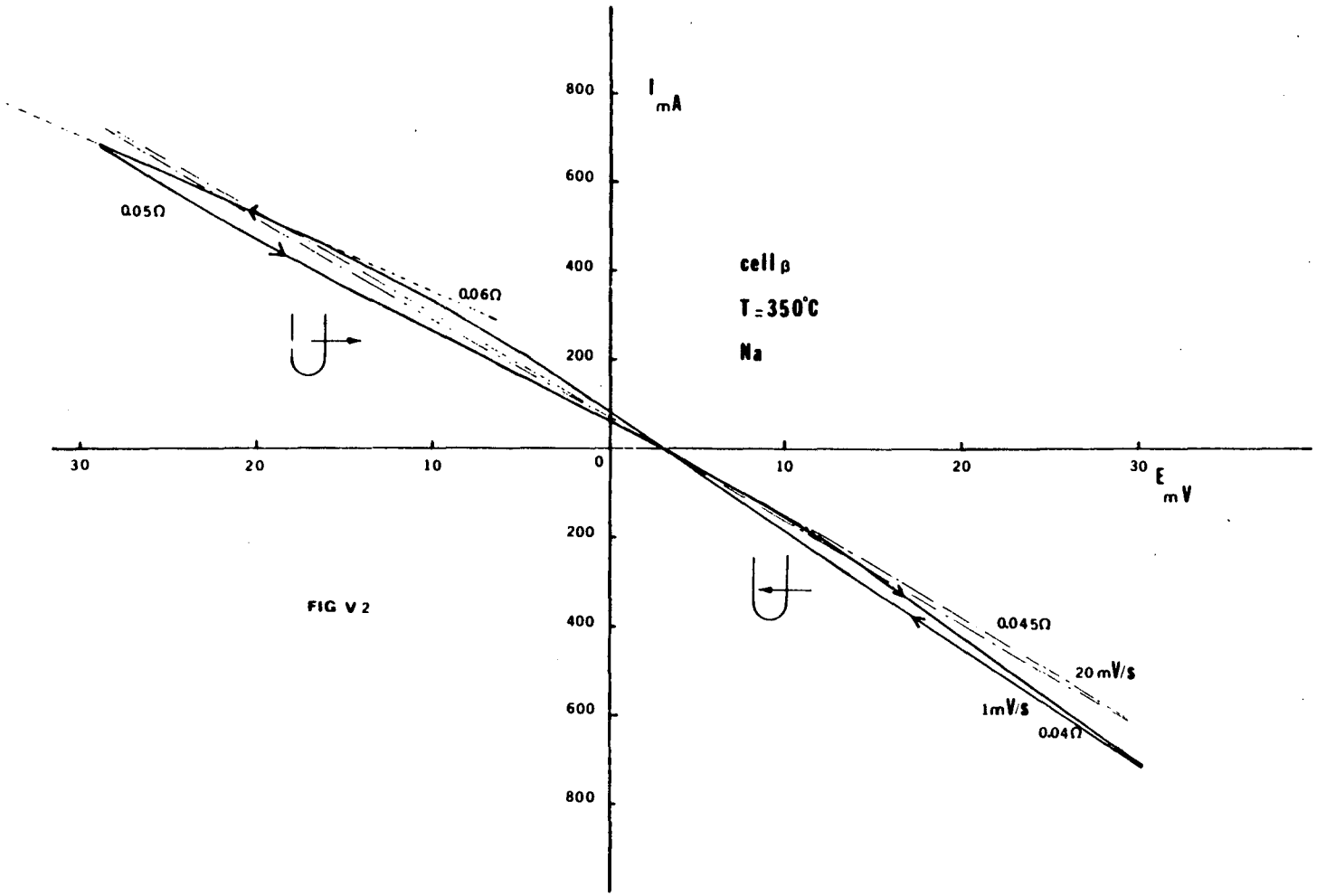

FIG V 2

XBL 845-1678

that the hysteresis, where it appears, also corresponds to an increase in resistance during discharge (sodium entering the $\beta''Al_2O_3$) as well as to a decrease in the resistance during charging (fresh sodium flowing in the tube). However, these effects are slight and do not involve any severe polarization or severe asymmetry.

B. Sodium with Sodium Oxide Na_2O (Fig. V3). (Cell γ) Some anhydrous Na_2O_2 is added at the bottom of the tube prior to any electrolysis. Na_2O_2 converts to Na_2O during the experiment, since $Na_2O_2 + Na \longrightarrow 2Na_2O$. This results in an increase of the overall resistance, but the shape of the voltammetry curves I/E is fairly similar to the ones obtained in the case of pure sodium and exhibits even less asymmetry than cell β.

C. Vanadium. A vanadium foil was added to cells α and β (Fig. V4, V.5). It is worth pointing out that the total surface area of foil was about 1/5 of the total surface of the tube wetted by Na.

In the case of cell α, a subsequent decrease in resistance was observed (from 0.1Ω without vanadium to 0.065Ω with vanadium). However, after a few days, the resistance increased again. The shape of the I/E curves is very similar to the ones obtained previously without vanadium foil.

In the case of cells β (which displayed a little more asymmetry than cells α for "pure" Na) the addition of vanadium didn't significantly decrease the overall resistance but did reduce the asymmetry.

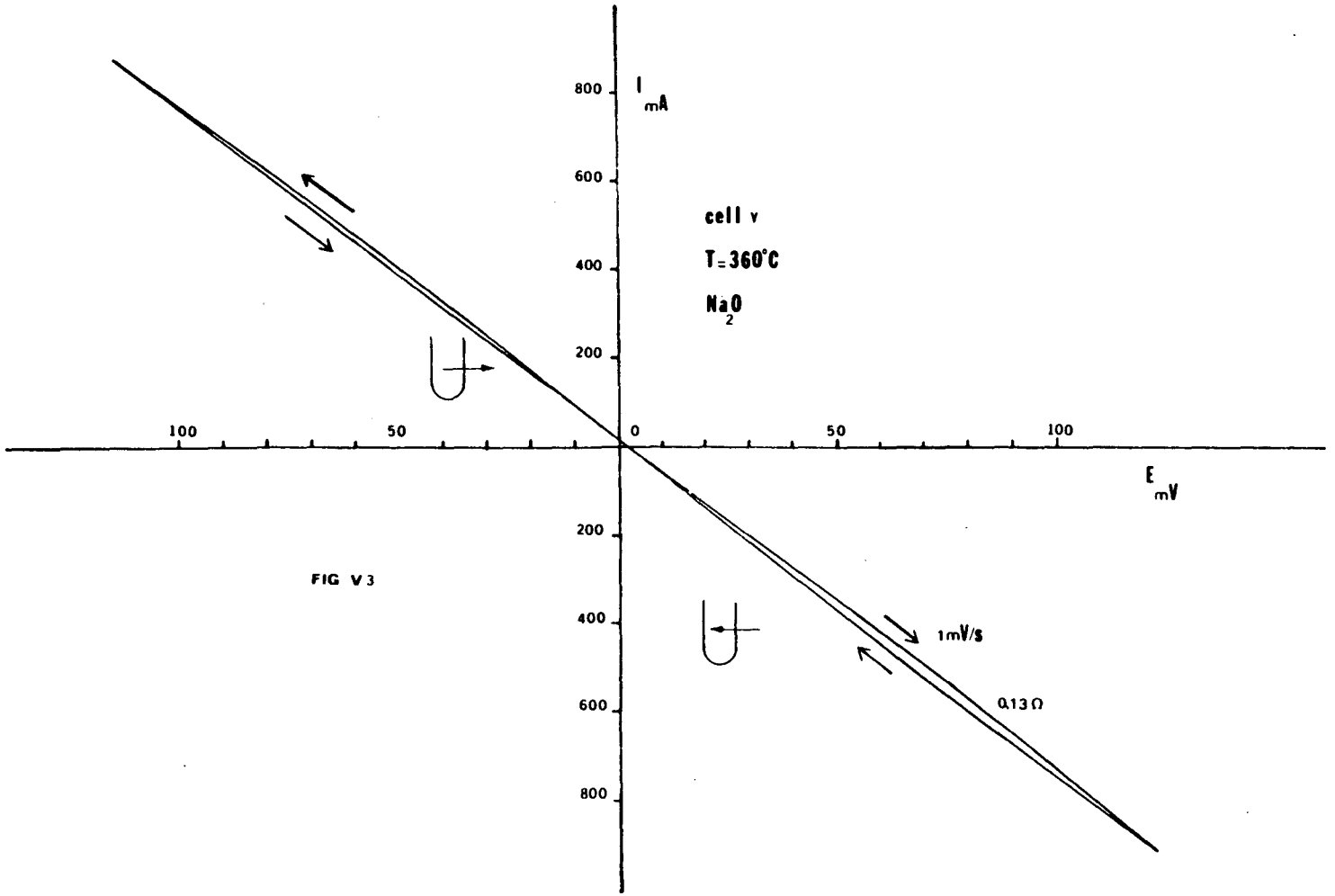

FIG V 3

XBL 845-1671

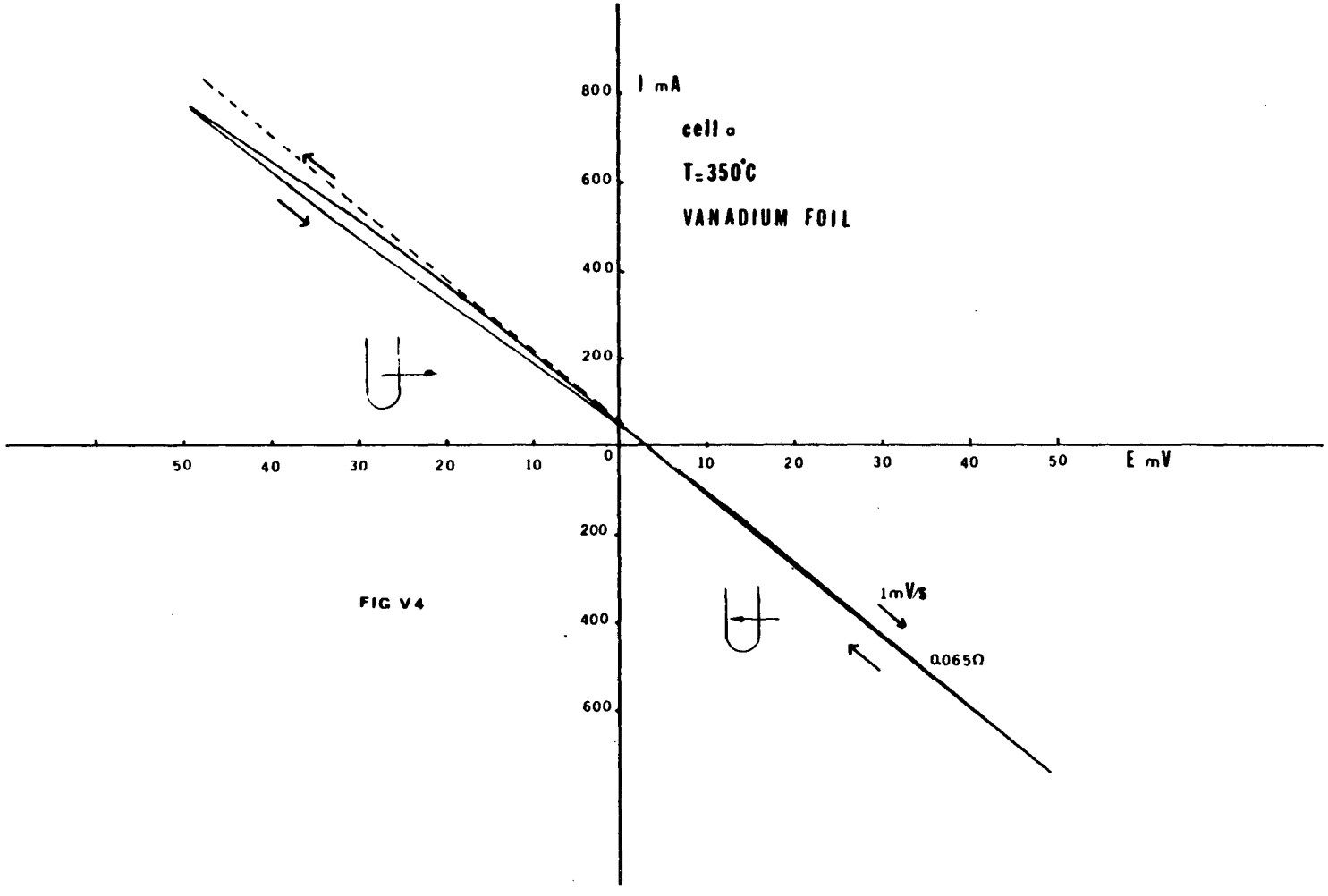

FIG V4

XBL 845-1677

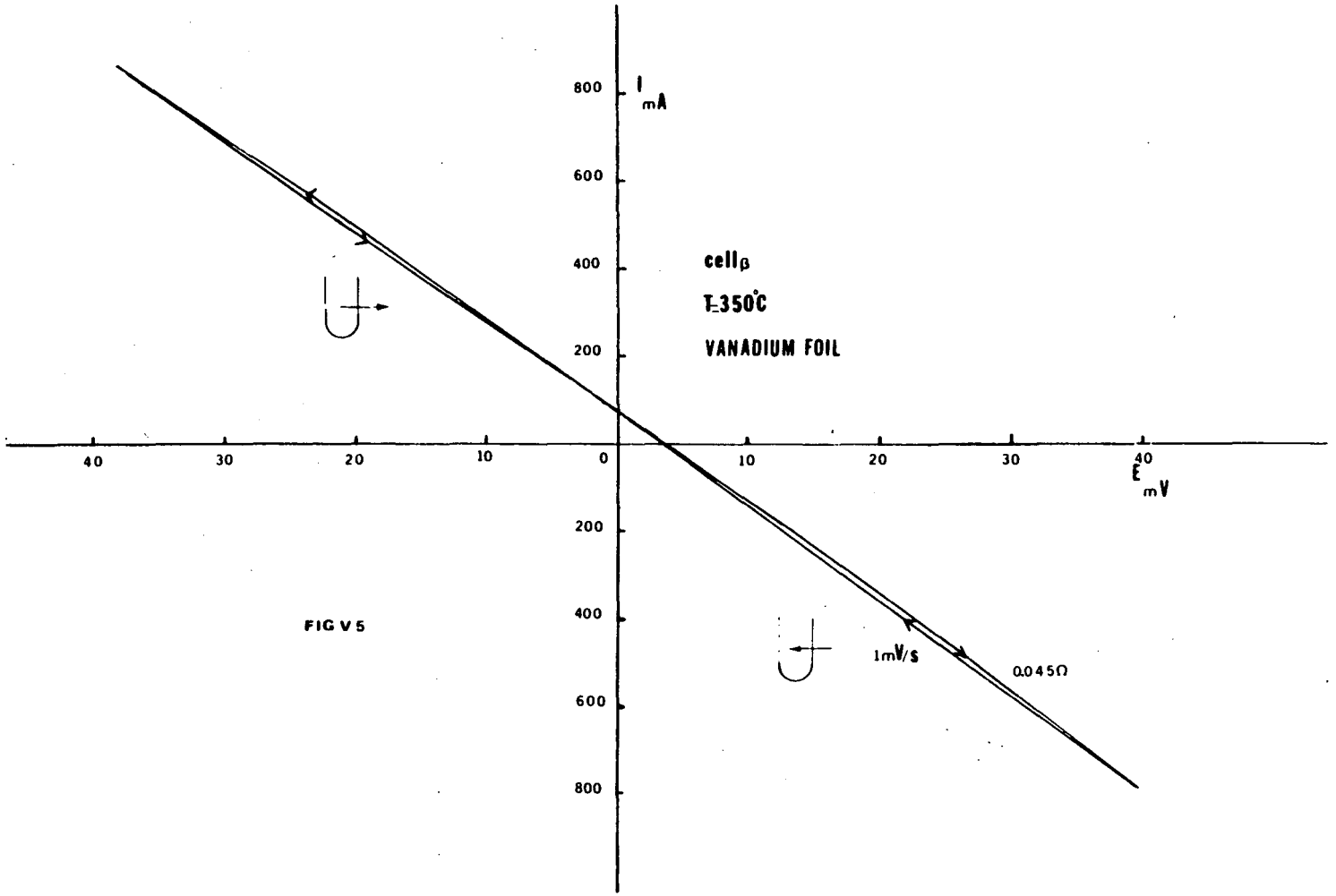

FIG V 5

XBL 845-1679

In conclusion of this study at 350°C, the shape of the I/E curves does not exhibit big differences between Na, Na_2O, Na/vanadium. The deviations from a Ohmic behavior, either hysteresis or asymmetry are really slight. However, the overall resistance does vary and exhibits an increasing value from Na/vanadium (the lowest) to Na and to Na + Na_2O (the highest).

V.1.2 T = 160°C

The I/E curves obtained in the three cases of pure Na, Na_2O and vanadium foil exhibited much higher deviations from Ohmic behavior than at 350°C.

V.1.2.A "Pure" Sodium

Cell α and β behaved differently from each other. Cell β exhibited the expected behavior: large asymmetry, with the resistance lower when fresh Na flowed in the tube than when sodium flowed out of the tube (for a scan rate of 2mV/s $R_d = 0.5\Omega$ and $R_c = 0.38\Omega$) (Fig. V.7). A time dependence was also observed, the asymmetry is larger for slower scan rates and the resistance for sodium flowing out of the tube is higher than the resistance for fresh sodium entering the tube.

Cell α exhibited an unexpected behavior (Fig. V6): an increase in the resistance for fresh sodium flowing in the tube and a decrease (slighter) of the resistance for sodium flowing out. Constant potential pulse measurements with the current recorded as a function of time (Fig. V.8), have shown that two effects are in fact superimposed. While at first, when fresh sodium is flowing in, the

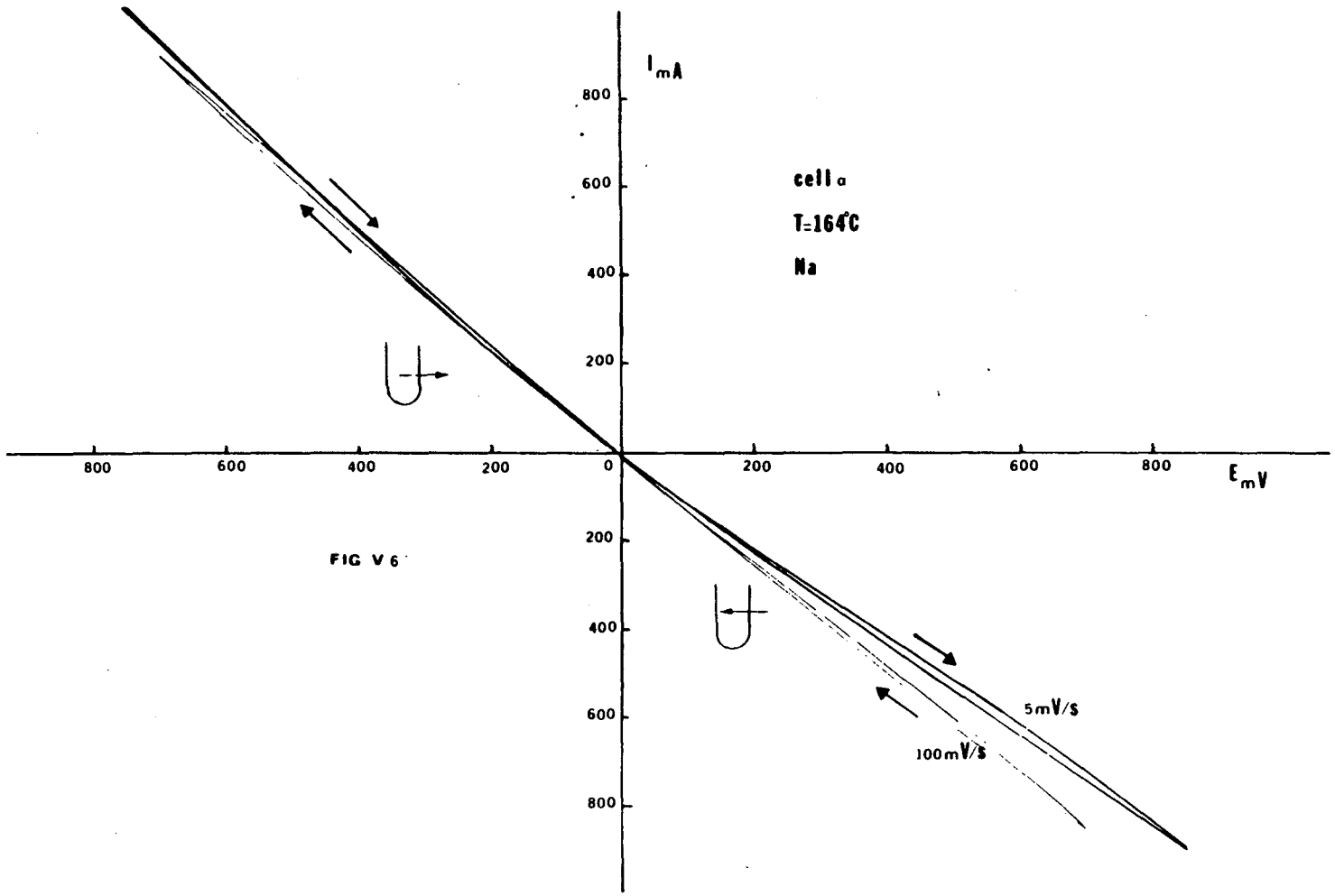

FIG V 6

XBL 845-1670

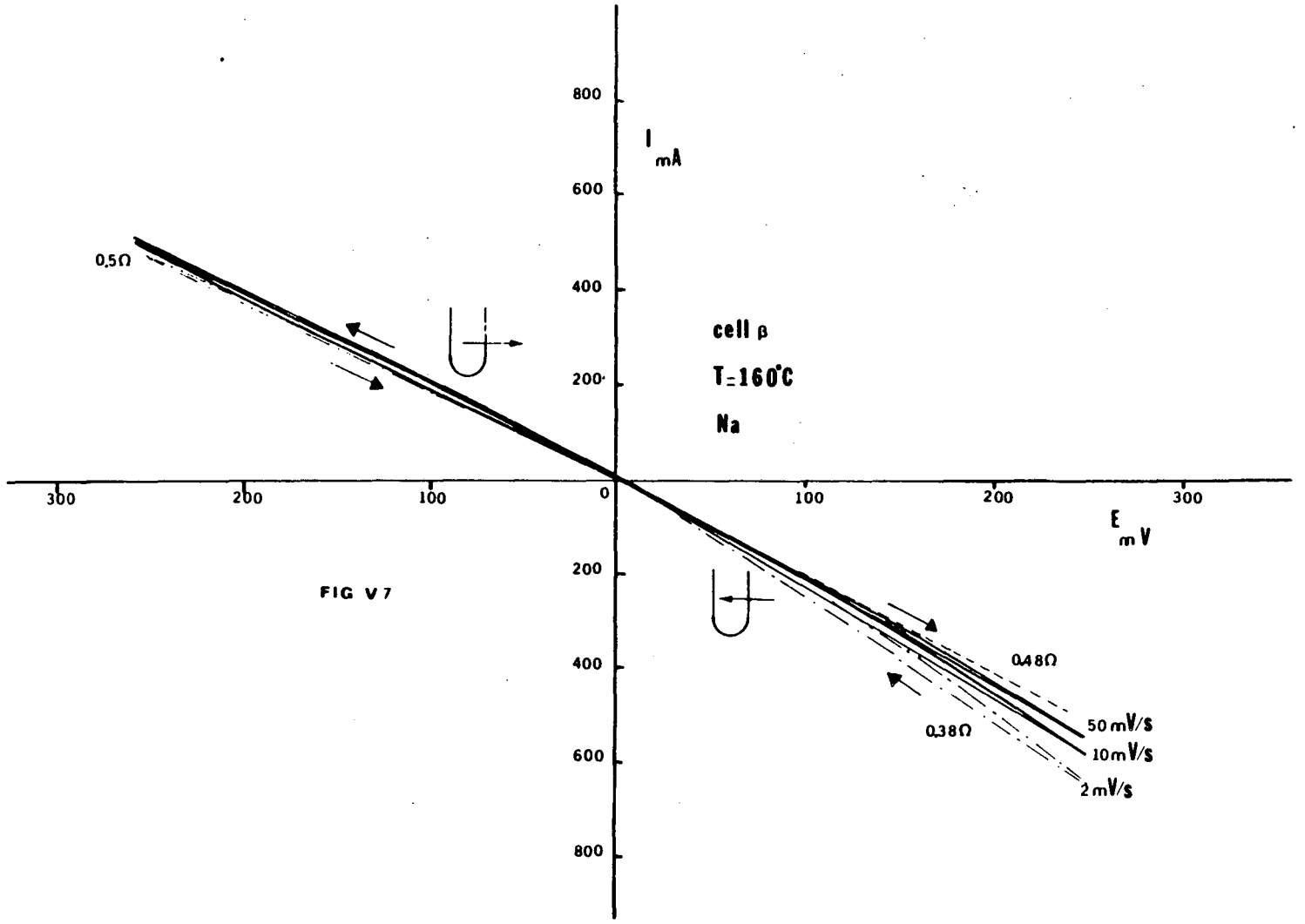

FIG V 7

XBL 845-1675

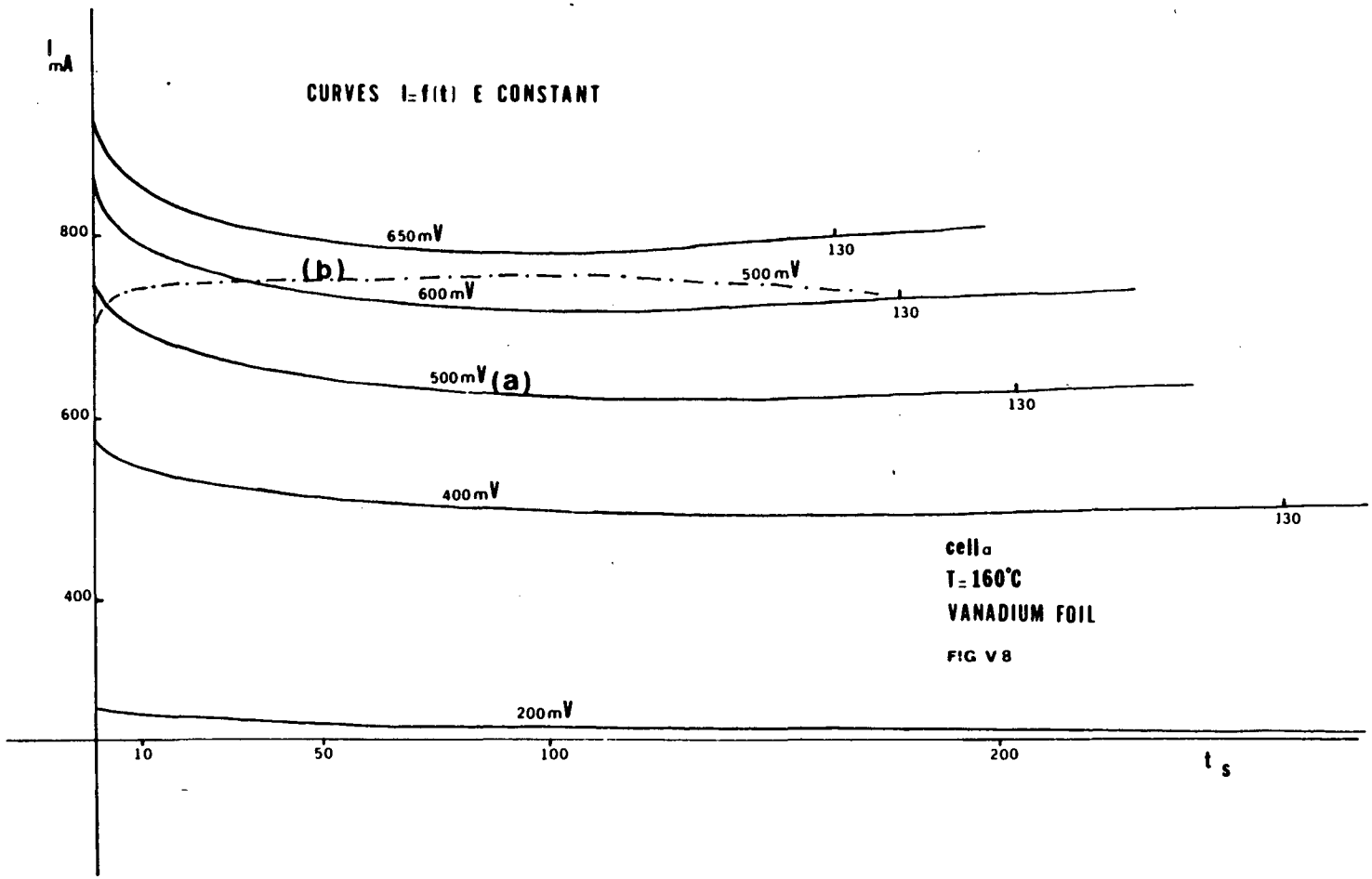

FIG V 8

XBL 845-1682

resistance increases, it decreases for a higher number of coulombs passed, which is the normal behaviour. When sodium flows out, the resistance first decreases and then increases again which is also the normal behavior. (The curve 500mV(a) corresponds to sodium flowing in the tube, curve 500 mV(b) corresponds to sodium flowing out of the tube). However, the phenomenon which occurs first is certainly not easy to clarify.

B. Na_2O (Fig. V.9, V.10, V.11). The presence of Na_2O first accentuates the asymmetry already encountered with "pure sodium". The resistance is higher for Na flowing towards the interface Na/β" than for sodium flowing into the tube. Here, a time dependence, ie, an influence of the scan rate, is observed with larger asymmetry for slower scan rates. The ratio R_d/R_c is equal to 1.9 at 240°C and 2.6 at 160°C. Na_2O causes a significant asymmetry at least with respect to what was observed so far.

The curve $\Delta I = f(E)$ obtained by suppressing the main Ohmic contribution evidences even more clearly the asymmetry and the time dependence effect.

C. Vanadium. In the case of cell β, the vanadium did not cause any noticeable change with respect to the cell without vanadium. The deviations from the Ohmic behavior are represented in Fig. V.12 in the form of a $\Delta I = f(E)$ curve where the main Ohmic contribution is suppressed. For cell α (Fig. V.13), which exhibited an unusual behavior, the introduction of vanadium foil brought a modification: the deviation from Ohmic behavior seems to be restricted to the part of the I/E curve corresponding to the fresh sodium flowing in the tube.

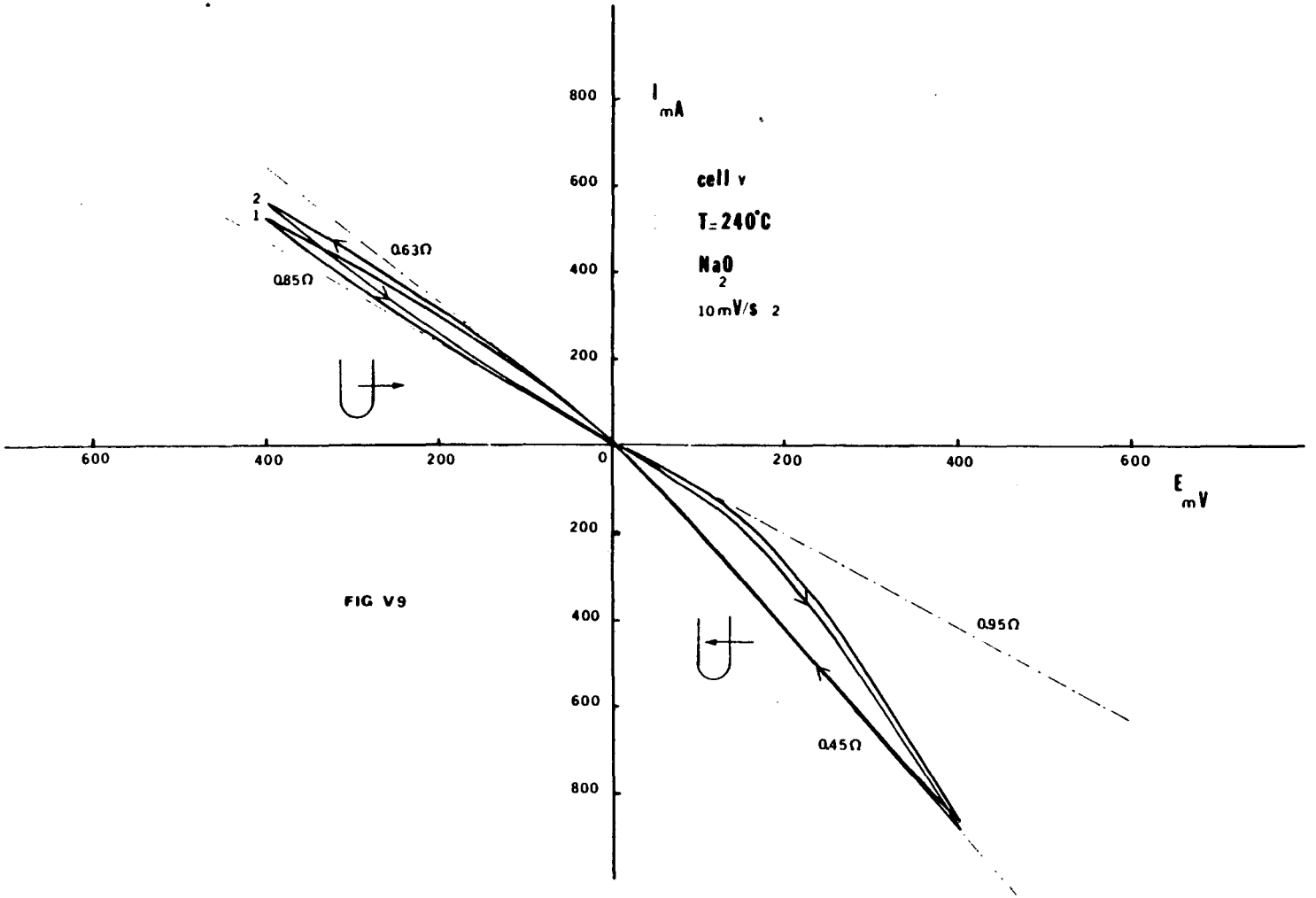

FIG V9

XBL 845-1680

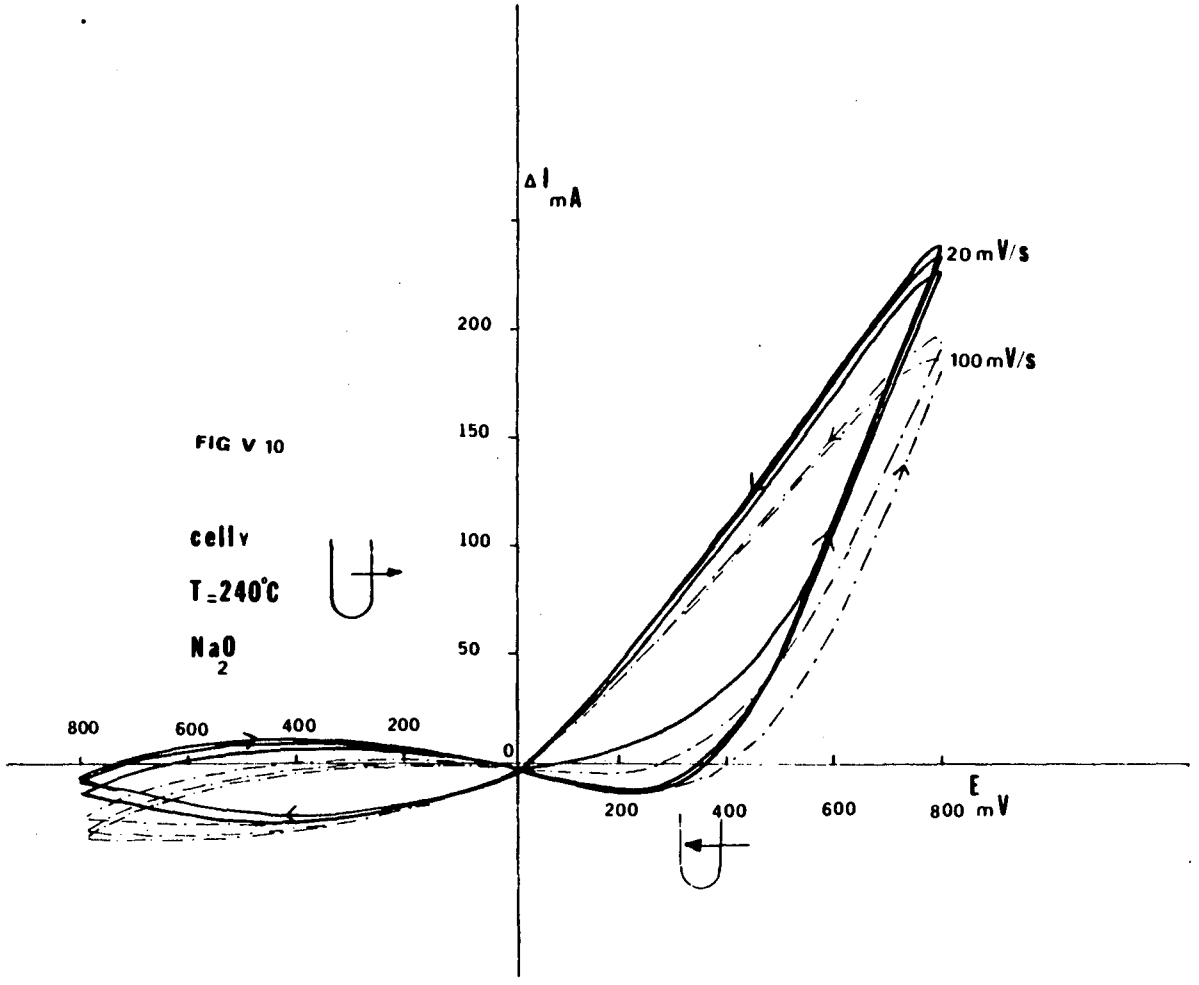
FIG V 10
cell v
T = 240°C
NaO2
ΔI mA
200
150
100
50
0
800
600
400
200
200
400
600
800 mV
E
20 mV/s
100 mV/s

XBL 845-1683

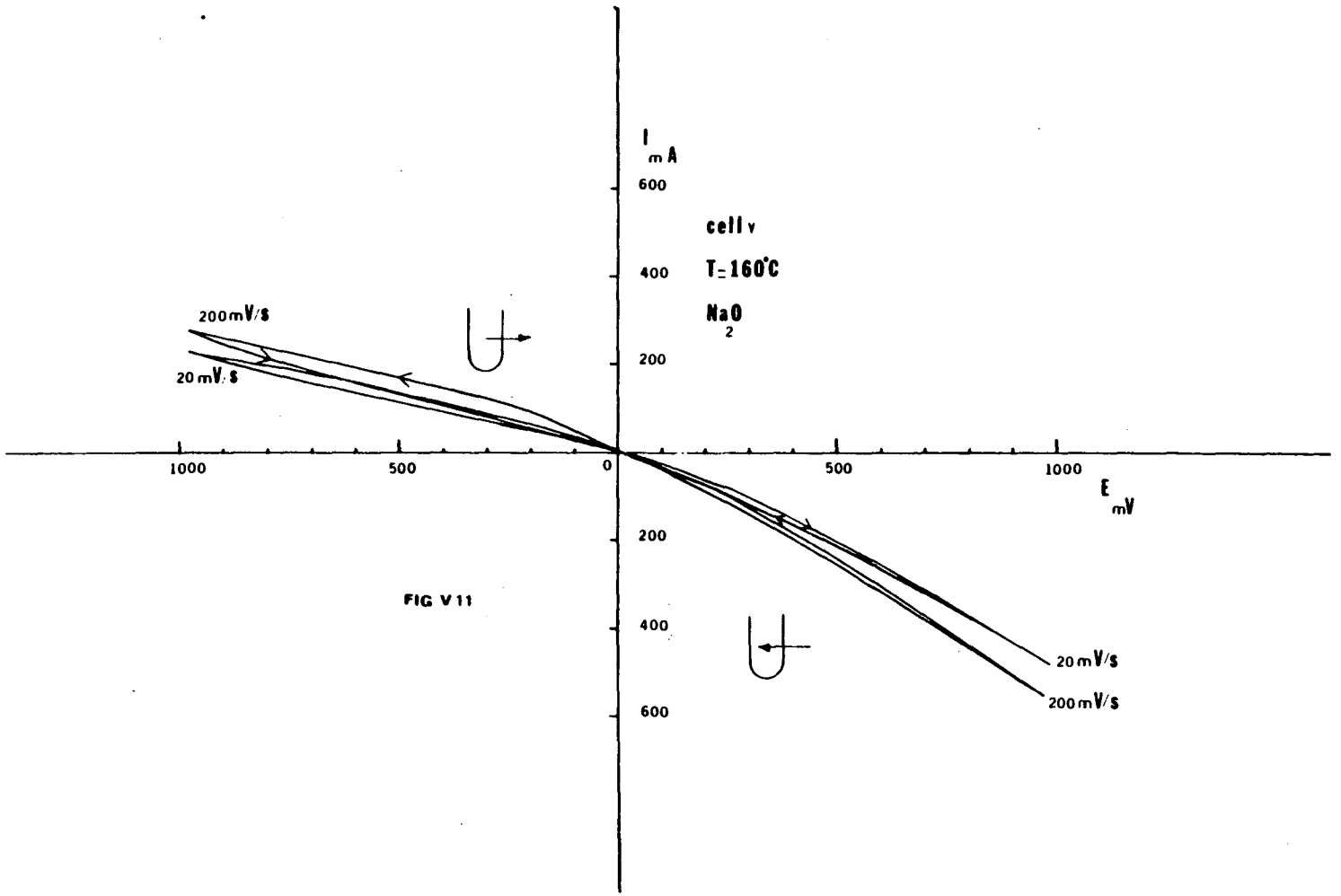

FIG V 11

XBL 845-1684

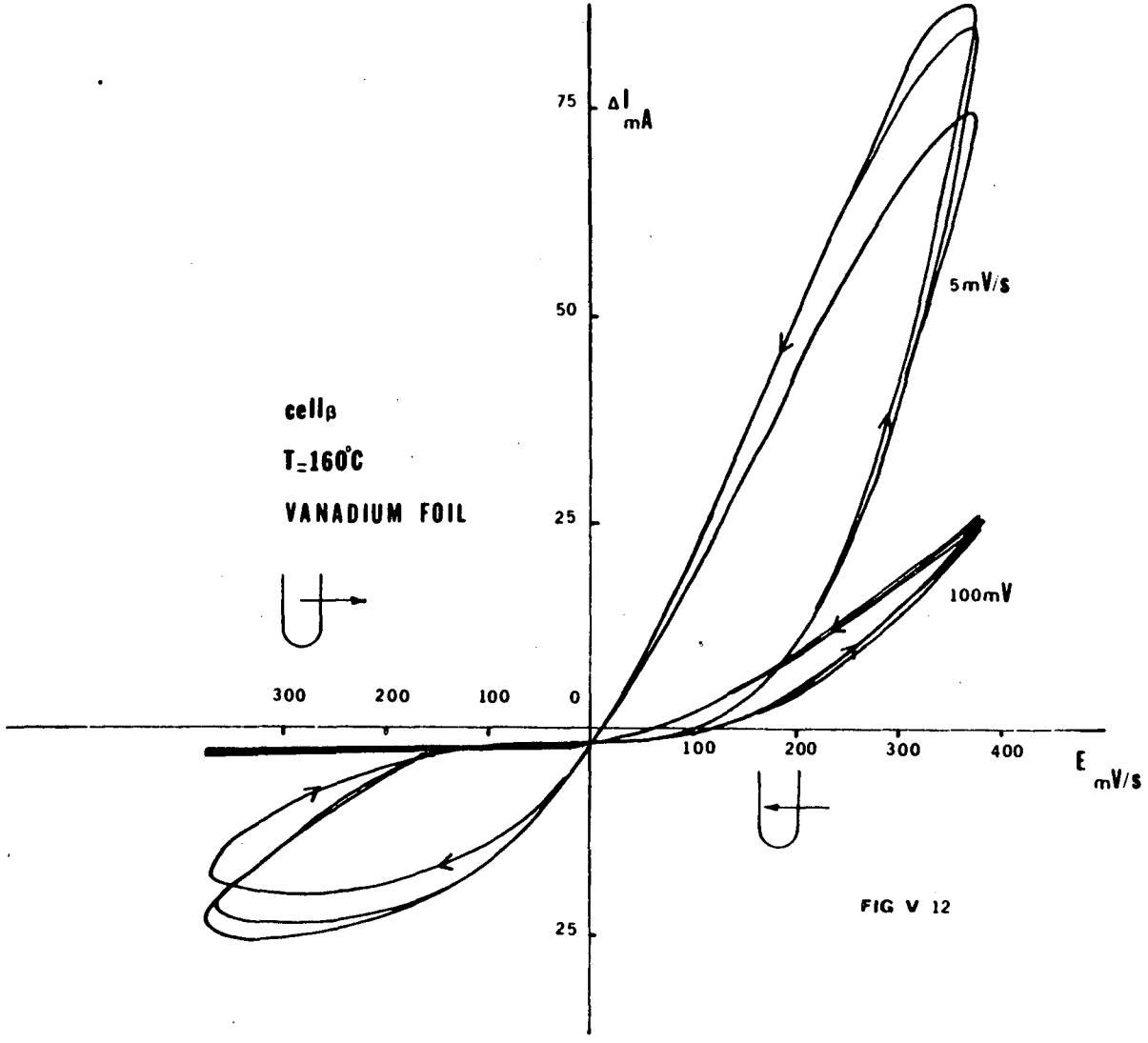

FIG V 12

XBL 845-1674

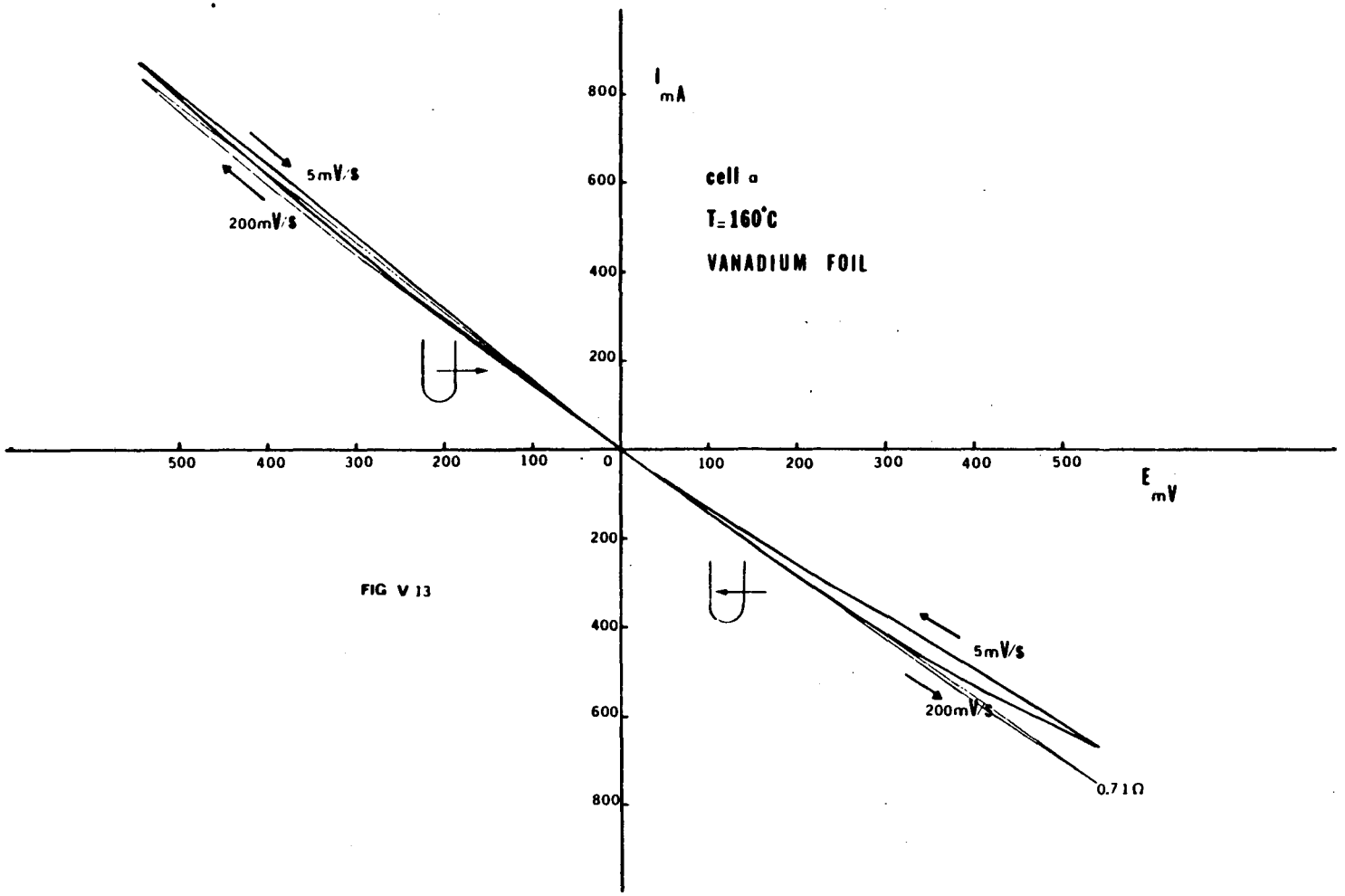

FIG V 13

XBL 845-1672

V.1.3 DISCUSSION

Naβ"Al_2O_3 is an Na^+ ionic conductor and behaves very much like a sodium selective membrane being rather impervious to other ions. More particularly, the O^{2-} ionic conductivity of Naβ"Al_2O_3 is negligible with respect to the Na^+ ionic conductivity (22). Therefore, the β"Al_2O_3 constitutes a blocking interface for any O^{2-} ions contained in the sodium flowing through the electrolyte. For sodium flowing out of the tube, the oxygen concentration at the inside interface of the tube will increase as the sodium goes through the electrolyte but the oxygen is stopped at the interface. When fresh sodium is drawn into the tube, the oxygen concentration will drop at the interface. A pile up/depletion model is proposed here to describe the role played by the oxygen; the model accounts for the deviations from the ohmic behavior observed in I/E curves. As the oxygen accumulates at the interface, a resistive layer builds up and a subsequent increase in the resistance is observed in the voltammetry curves, whereas the depletion of oxygen when fresh Na is flowing in is associated with a decrease in the resistance. As a first approximation, except in one case, the asymmetry and the hysteresis observed in the three cases "pure" Na, Na_2O and vanadium foil fit this model (cf. β at 160°C).

Schematically the oxygen concentration profiles should have a shape close to the one represented in Fig. (V.14).

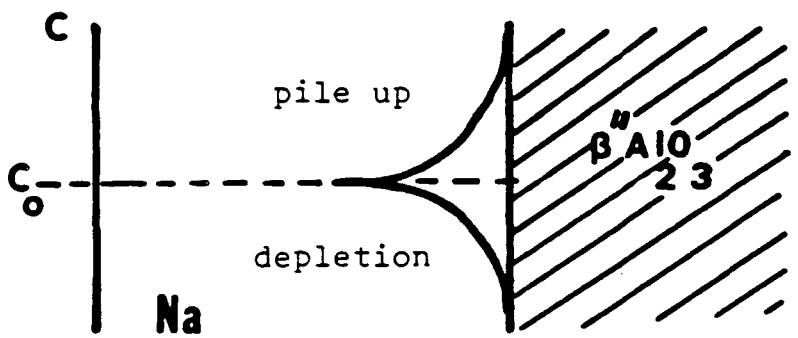

Fig.V.14 Oxygen concentration profiles at the interface Na/ Al_2O_3
c:oxygen concentration
c_o: oxygen concentration in the sodium.

In terms of this fairly simple model, the idea consists then in varying the activity of the oxygen either by adding some sodium oxide or some vanadium foil. The tube filled electrolytically with Na and without any additives is taken as a reference, although a partial coverage of the tube by Na_2O may be present (e.g. as a result of H_2O adsorption). Nevertheless, when Na_2O is added at the bottom of the tube prior to any electrolysis, the oxygen supply is undoubtly greater than in the case of "pure" Na and, as expected, the formation of an Na_2O oxide layer contributes to an increase in the resistance, so that

$$R_{cell}Na_2O > R_{cell} \text{ pure Na}$$

On the other hand, the introduction of vanadium in the tube already filled electrolytically causes a decrease in the resistance. The most probable explanation is that vanadium scavanges the oxygen and removes the Na_2O layer present at the surface. It is worth pointing out that after a few days the resistance increases again. Thus, more consideration needs to be given to the quantity and the form under which vanadium is introduced: Foil, powder or preferably a sponge form. In both cases (cell α and β) the surface area of the vanadium foil was lower than the one of $\beta''Al_2O_3$ wetted by Na. This difference may explain why the decrease in resistance of cell α was only temporary. The initial resistance of cell β is also much lower than that of cell α and the difference in the interface β''/Na surface area cannot account entirely for this difference. One

possibility is that the surface of $\beta''Al_2O_3$ in cell β was much cleaner than in cell α, therefore, the vanadium didn't cause a significant decrease in the resistance because the initial oxide layer was less important.

The use of vanadium would certainly be of very high interest for the Na/S battery, since decreasing the interfacial resistance improves the efficiency of the battery as well as its lifetime. Vanadium would not be the only possibility, other transition metals such as titanium, manganese would have the same effect.

The $\Delta I = f(E)$ (Fig. V.10, V.12) curves for which the main Ohmic behaviour is suppressed show clearly the asymmetry but also the temperature and time dependence effect. These two effects may be explained on the basis of this pile up/depletion model.

Time Dependence Effect. At 350°C as well as at 160°C, higher asymmetry and hysteresis are observed with slower scan rate. Usually when the electrochemical process involves a rate limiting step, diffusion limitation for example, deviations from the equilibrium state increase with the scan rate. In our case Na is the electroactive species whereas the oxygen is not electrochemically active. At slower scan rate, more sodium is passed through the electrolyte and the quantity of oxygen to be piled up is more important. Therefore the variations in the resistance should be more noticeable.

Temperature dependence effect. The temperature effect may be explained in terms of kinetics. The diffusion coefficient of the oxygen in molten sodium is temperature dependent and is obviously

smaller at 160°C than at 350°C. The oxygen is acted on by two driving forces: one is the flow of sodium for which velocity and direction are determined by the current density and which is T independent; the other is a gradient in the chemical potential. When the oxygen piles up, its chemical potential increases and therefore the oxygen diffuses back to the bulk of liquid sodium. This second effect depends on the self diffusion coefficient of the oxygen and is temperature dependent. At lower T, the pile up is less counter balanced by the self diffusion.

In addition, the oxide layer happens to form more easily at lower T as the solubility product of Na_2O is decreasing (or respectively to dissolve).

This demonstrates, if necessary, the importance of this study at lower temperatures even if they don't belong to the range of operation of a Na/S battery. It provides a better understanding of the processes occurring at the interface and of the oxygen role.

There is still an unclarified point in the case of cell (α) (Fig. V.6, V.13) at low T where another phenomena is superimposed as shown by the curves I=f(t) (Fig. V.8). The pile up depletion model accounts for most of the deviations observed, but is certainly an approximation to the complexity of these processes.

In conclusion, it has to be pointed out once again that at 350°C, the normal operating temperature of the battery, the deviations from the Ohmic behavior are slight. The potential of the working electrode is directly related to the activity of the electroactive species,

i.e., the sodium. The oxygen is not the electrochemically active species and even if significant oxygen concentration changes occur at the interface, they don't affect the sodium activity very much. Therefore, large overvoltages won't be observed. But on the other hand, the formation or the dissolution of an oxide layer will result in a decrease (respectively an increase) of the overall resistance. This result was clearly demonstrated by the addition of Na_2O which increases in the resistance, whereas the addition of vanadium leads to a decrease in the resistance. The asymmetry was much more accentuated at lower temperature in all cases, but more drastically with Na_2O. Oxygen has always been accounted in the literature for these deviations from the Ohmic behavior, these experiments confirm the fact that specifically the oxygen has a deleterious effect and is responsible for it. However, only asymmetry and hysteresis were observed, no electrochemical waves were observed in the voltammetry experiments.

IV.2 Water

To study water contamination, as well as in the case of other impurities, the usual three electrode electrochemical set up was used. Therefore, an ohmic drop of the order of 0.03Ω was introduced at the working electrode and may have concealed slight deviations from the ohmic behaviour. Nevertheless the study at low T is valid as the resistances involved are much higher (1-2Ω).

IV.2.2 Experimental Results

The βAl_2O_3 tube was exposed to air for three weeks. Some problems were encountered with the reference electrode which seemed to

suggest that a partial failure or dendritic penetration by Na on the inside interface in a mode I fashion had occurred. However, after dismantling the cell, no cracks could be found.

At 350°C, an Ohmic behavior was observed for both interfaces Fig. V.16, V.17). At 160°C deviations very similar to the ones obtained in the case of the oxygen alone were evidenced on the outside interface.

IV.2.2 Discussion.

With the restriction that only the outside interface could be studied, the low T experiments show a type of polarization very similar to the one due to Na_2O only. The sodium of the outside compartment contains some Na_2O, therefore the only conclusion that can be drawn is that the presence of water doesn't introduce very significant changes with respect to Na_2O alone as far as the polarization curves are concerned.

However, the severe darkening undergone by the tube shows that a significant degradation process has taken place. Fig. V.15 shows the $\beta''Al_2O$ tubes of cells contaminated by KCl, H_2O, CaO, $CaCl_2$ and Ca. The tube that has been water contaminated appears almost black. The cross section of the tube shows that a more darkened layer has also developed near the surface.

IV.3 Other Impurities Ca,K

The influence of Ca in different forms was investigated. CaO, $CaCl_2$ and Ca metal. Potassium was introduced in the form of KCl. Only partial results are presented here.

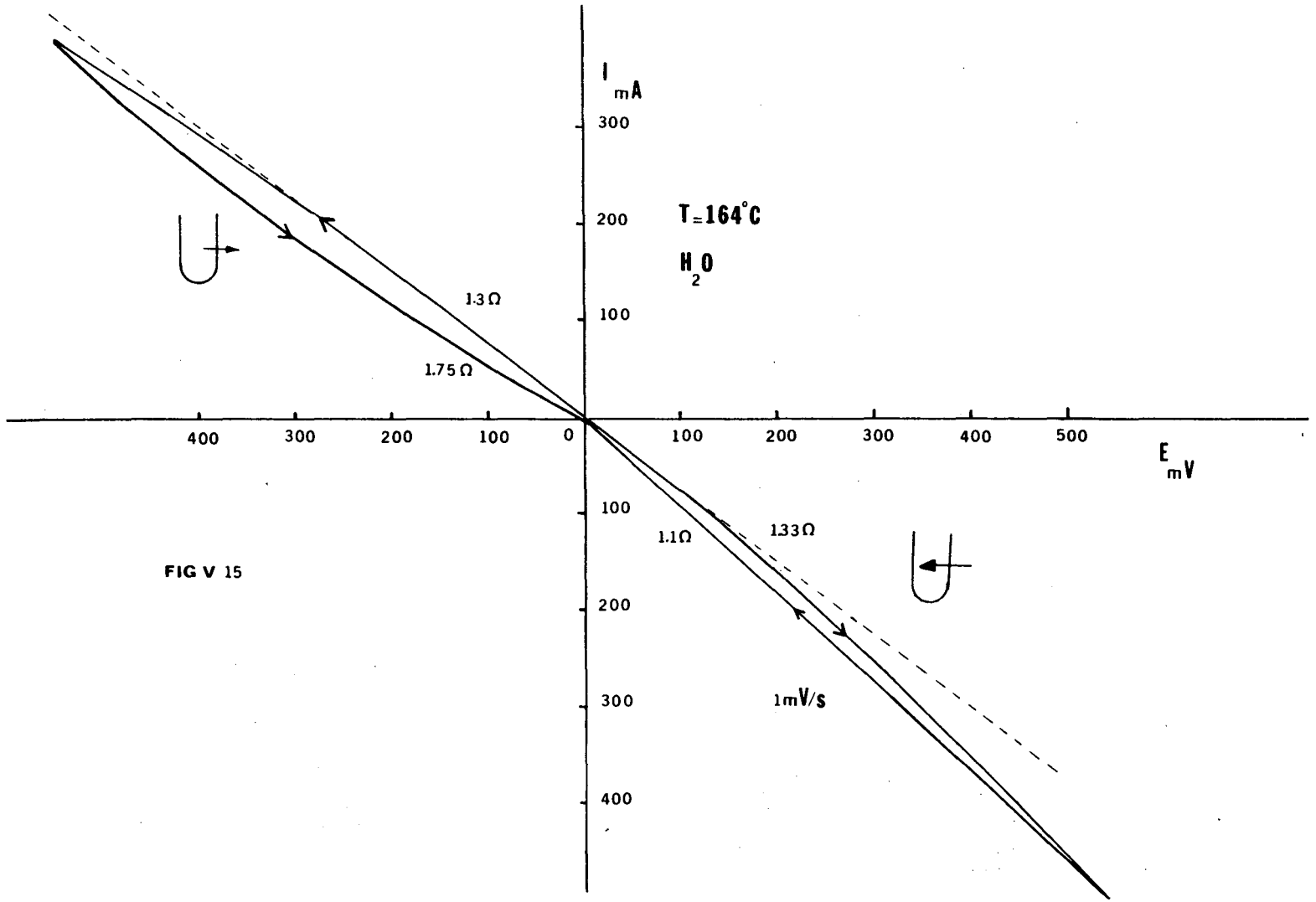

FIG V 15

XBL 845-1673

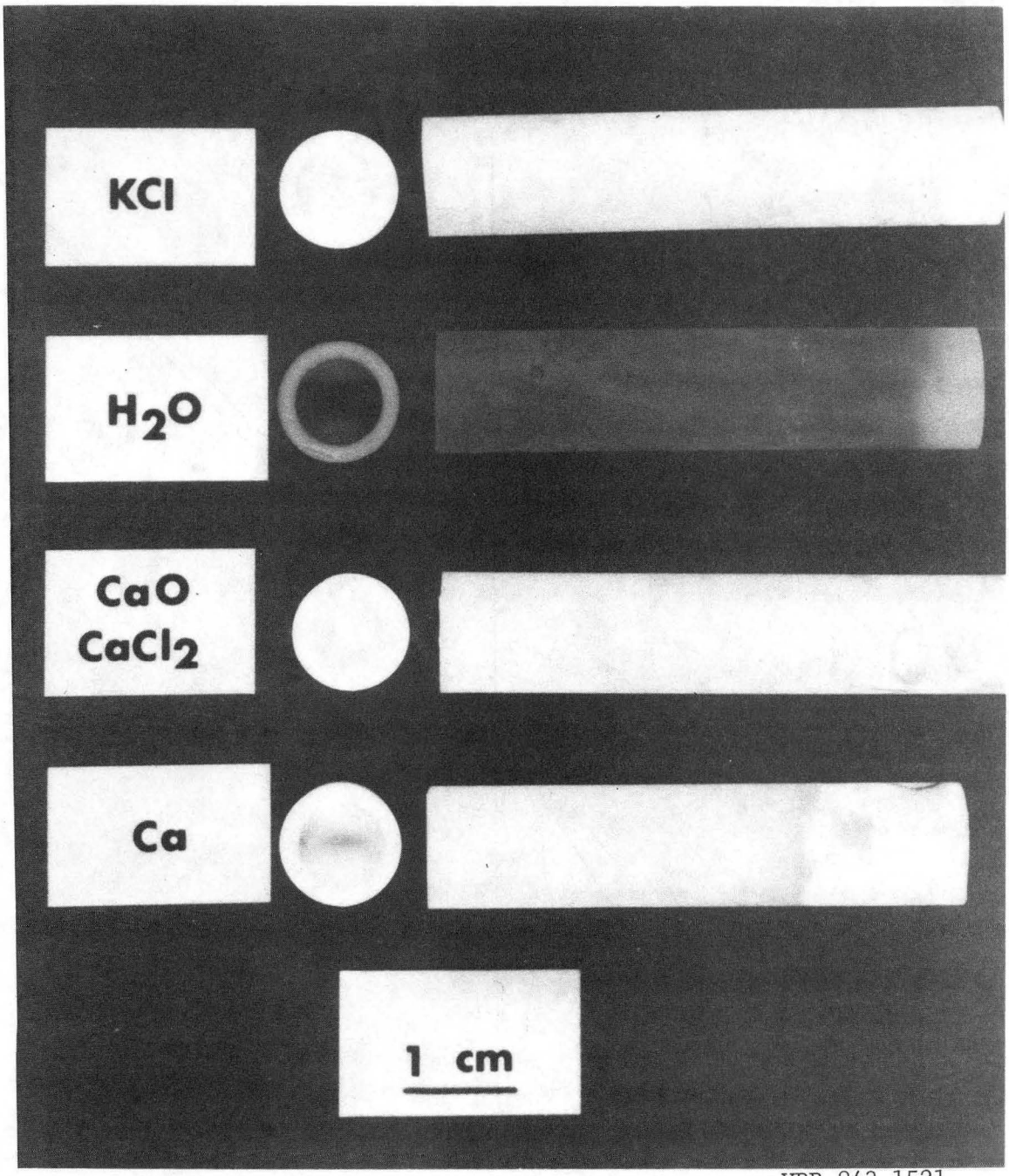

XBB 843-1521

Fig. V.16. β'' alumina tubes after cycling.

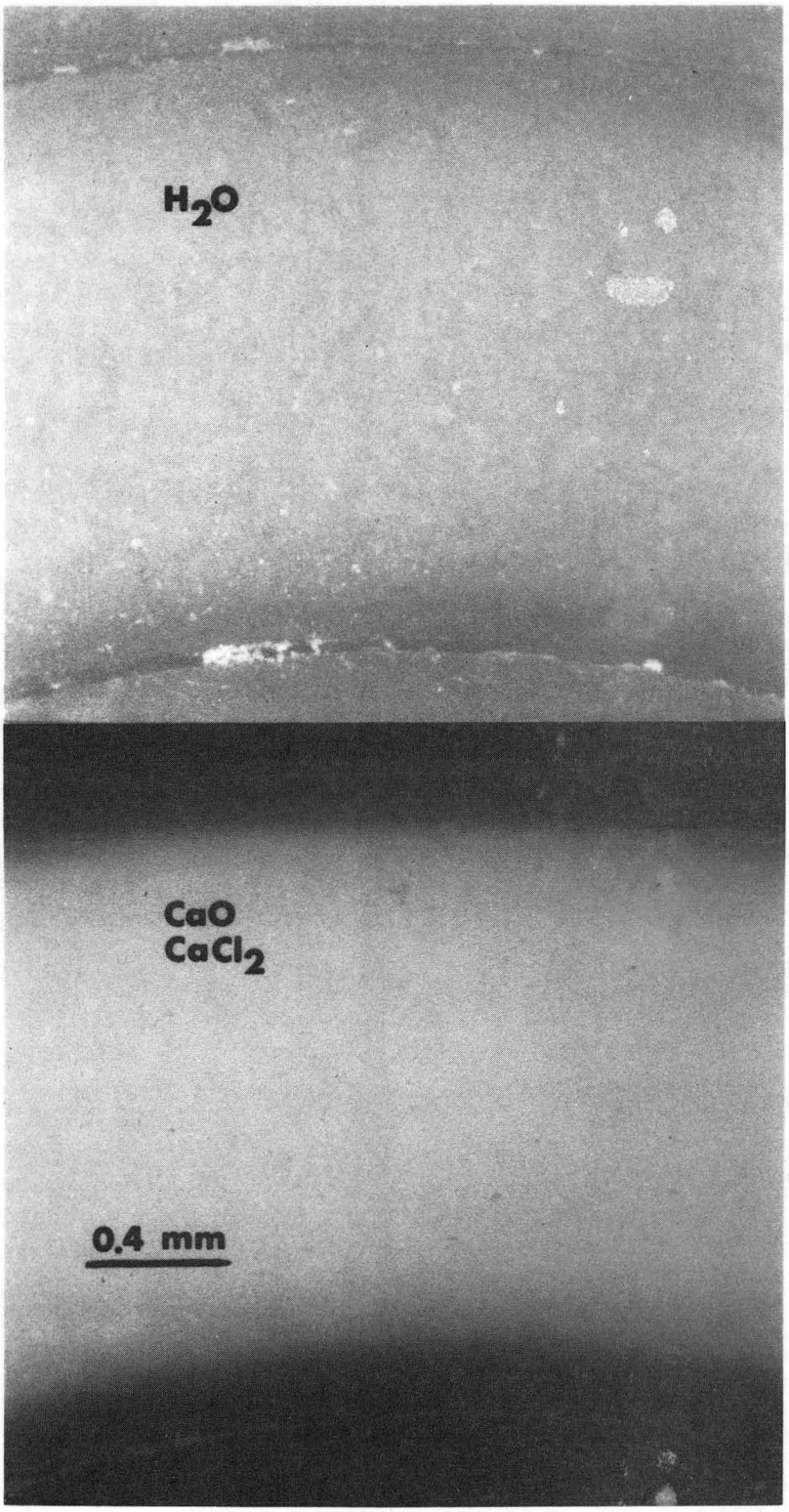

XBB 843-1520

Fig. V.17. Cross section of H_2O and CaO $CaCl_2$ contaminated tubes.

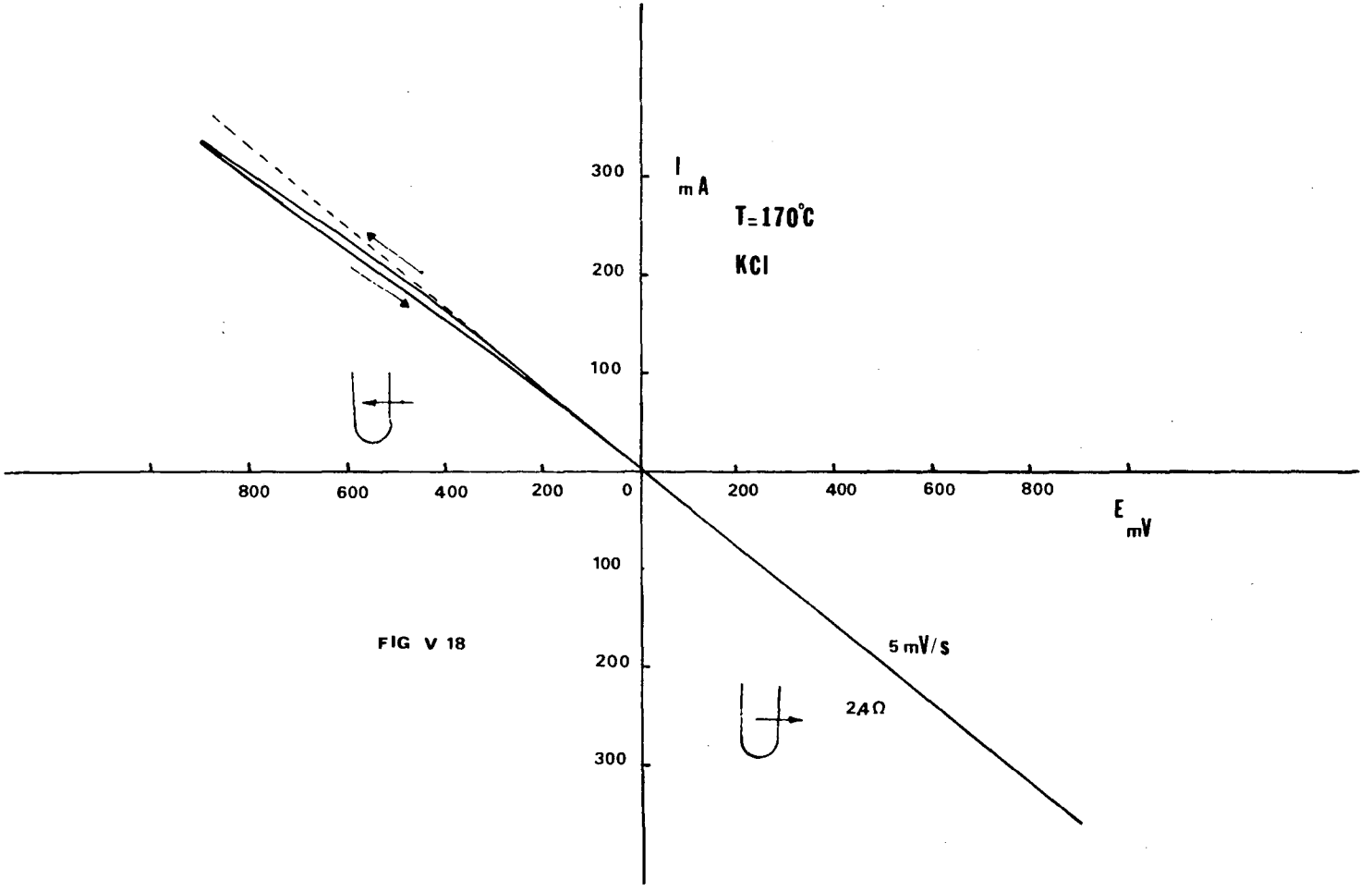

FIG V 18

XBL 845-1681

Table I

	Number of Coulombs	Surface area cm^2	R_T = 360°C	R_T = 360°C Vanadium Foil	R_T = 160°C	R_T = 160°C Vanadium Foil
Cell α	4700	5.6	0.1Ω non-asymmetry very little hysteresis	0.07 Ω more hysteresis and assymetry. The R increases back up after a few days 0.09Ω	1Ω unexpected deviation from the ohmic behavior	0.7Ω unexpected derivations from the ohmic behavior
Cell β	5600	6.6	0.045Ω assymetry hysteresis	0.047Ω less asymmetry	0.4-0.5Ω Pile up/depletion clearly evidenced	0.4-0.5Ω unexpected deviations from the ohmic behavior
Cell γ Na_2O	5700	6.7	0.13 Ω little hysteresis, no asymmetry		very large asymmetry,	

IV.3.1 Experimental Results

CaO = CaO was added at the bottom of the tube prior to any electrolysis. I/E curves at 350°C showed an ohmic behavior, the expected tremendous increase in the resistance was not observed even when the cell was left several days without passing any current or cycled at low current density. The tube didn't fail.

$CaCl_2$ = As CaO didn't prove to have any noticeable effect, some $CaCl_2$ was added in the same cell. No increase in resistance was evidenced. The same kind of problems with the reference electrode as for the water contaminated cell was encountered. No cracks were found on the tube (Fig. V.16).

Ca Metal = Some pellets of Ca metal were added with chuncks of sodium of the same purity as the Na used in the outside compartment. The tube was not filled electrolytically. No significant increase in the resistance was observed while the cell was cycled and the tube did not fail. At 350°C the cell exhibited an Ohmic behavior.

KCl = Some KCl was added inside the tube but also in the outside (Fig. V.17) compartment so that its influence can still be studied on the outside interface in case of a problem with the reference electrode, which appeared to be the case. At 350°C, an ohmic behavior was observed on both interfaces, at 160°C I/E curves presented on an asymmetric behavior very similar to the one observed in case of water contamination.

IV.3.3 Discussion

At the first sight these experimental results are puzzling in the sense that Ca, and to a smaller extent K, are known to be among the most damaging impurities. (Resistance increases of the order of 10-20 times in the case of Ca (36).) A sharp increase in the resistance was expected here also, especially when contaminated Na is flowing into the electrolyte. However, it must be pointed out that Ca or K are added on the sodium side whereas in the experiments just mentioned, they were added at the sulfur side, or Ca was already present in the solid electrolyte itself. The solubility of CaO, Ca, CaCl, or KCl in Na is very low, therefore we are very far from the ionic exchange conditions for which the solid electrolyte is immersed in the corresponding molten salt, usually at temperature higher than 350°C. In other words, we have no indication that Ca^{2+} or K^{+} are actually entering the structure. In addition, recent ionic exchange experiments performed by Whitmore showed that for very small fraction of Na^{+} exchanged by Ca^{2+}, the conductivity first increases (increase in the number of vacancies by replacing two Na^{++} by one Ca^{2+}), before decreasing sharply for further rates of exchange (33).

V. CONCLUSIONS

The present study has been mainly focussed on the effect of the oxygen in the electrochemical behavior of the Na/β" alumina interface. At 360°C under a low current density, β"Al_2O_3 exhibits an ohmic behavior. The oxygen does not have much effect.

For higher current densities, slight deviations from the ohmic behavior, asymmetry and hysteresis could be observed. These deviations are accentuated at lower T (160°C) for kinetic reasons.

By studying the effect of Na_2O and of vanadium, a model for the role of the oxygen has been presented. β"Al_2O_3 behaves like a blocking interface for the oxygen, which either piles up or is swept away from the interface according to the flow direction of Na. An increase in interface resistance is associated with the pile up as well as a decrease in resistance with the depletion.

The use of vanadium to clean the β"Al_2O_3 surface from the oxygen would certainly improve the performances of an Na/S battery at least by reducing its resistance. Further investigations among other transition metals such as manganese or titanium would be highly interesting.

Ca or K didn't cause drastic increases in the resistance. A more detailed study would nevertheless be necessary, using a four probe measurement.

REFERENCES

1. J. T. Kummer, Progress in Solid State Chemistry 3, $\beta/\beta''Al_2O_3$, p. 168.

2. J. C. Wang, Charge compensation mechanism in βAl_2O_3. J. Chem. Phys. 73(11), 1980, p. 5786-5795.

3. J. Tally, C. Lasne, Y. Lozennec, Y. le Cars and P. Margotin. Study of a βAl_2O_3 electrolyte for Na/S battery. Jnl. Electrochem. Soc., Vol. 120 (Oct. 1973, p. 1296.

4. D. Wolf. On the mechanism of diffusion in sodium β alumina. Chem. Solids. Vo., 40, p. 757-773.

5. J C. Wang, J. B. Bates, N. J. Dudney and H. Engstrom. Study of β and β" by means of potential energy calculations. Solid State Ionics 5 (1981), 35-40.

6. U. Strom. Review disorder phenomena in βAl_2O_3. Solid State Ionics 8 (1983), 255-279.

7. J. D. Jorgensen, F. J. Rotella and W. L. Roth. Conduction plane and structure of Li Stabilized Na^+ $\beta''Al_2O_3$, a powder neutron diffraction study. Solid State Ionics 5 (1981), 143-146.

8. W. L. Roth, R. E. Bennenson, V. K. Tikku. Li and Mg stabilized βAl_2O_3. Soli State Ionics 5: 163-166 (1981).

9. J. B. Bates, H. Engstrom, J. C. Wang, and B. C. Larsen. Composition ion-ion correlations and conductivity of $\beta''Al_2O_3$. Solid State Ionics 5 (1981), p. 159-162.

10. J. D. Hodge. Kinetics of the β" to β transformation in the system Na_2O/Al_2O_3. Jrnal. Am. Ceram. Soc. Vol. 66, No. 3, p. 166.

11. EPRI Report EM-2160, Improved beta alumina electrolytes for advances storage batteries.

12. L. A. Feldman and L. C. DeJonghe. Initiation of mode I degradation in Sodium beta alumina electrolytes. Jrnl. of Mat. Sciences 17 (1982), 517.

13. R. D. Armstrong, T. Dickinson, I. Turner. Electrochem. Acta 19, p. 187 (1974).

14. R. H. Richman and G. J. Tennenhouse. Model for degradation of ceramic electrolytes in Na/S batteries. Jrnl. Am. Ceram. Soc. 58, p. 63 (1975).

15. L. C. DeJonghe, L. Feldman and A. Buechele. Failure modes of Na Beta alumina. Solid State Ionics (1981), 267-270.

16. C. V. Virkar, L. Viswanathan and D. R. Biswas. On the deterioration of $\beta''Al_2O_3$ ceramics under electrolytic conditions. Jrnl. of Materials. Sci. 15 (1980) 302-308.

17. L. C. DeJonghe. Transport number gradients and solid electrolyte degradation. Jrnl. Electrochemical Society, 129 (1982), p 752.

18. V. Virkar, et al. Enhancement of ionic conductivity of $\beta''Al_2O_3$ by selenium treatment. United States Patent 4, 407, 912 Oct. 4, 1983.

19. L. Viswanathan and A. V Virkar. Wetting characteristics of sodium on $\beta''Al_2O_3$ and on Nasicon. Jrnl. of Mat. Science 17 753-759 (1983).

20. Gibson. International Power Sources Symp. 6 (1977), 673.

21. A. Gibson. A study of the electrode interface formed between sodium metal and beta alumina solid electrolyte. Power Sources 6, Ed. D. H. Collins p. 673, Academic Press, 1977.

22. L. C. DeJonghe, A. Buechele and M. Armand. Oxygen interstitial transport and chemical coloration in sodium βAl_2O_3. Solid State Ionics 9,10 (1983), 165-168.

23. A. C. Buechele (Ph.D. Thesis), Factors contributing to the breakdown of sodium beta alumina (May, 1982).

24. J. B. Bates, N. J. Dudney, J. C. Wang and W. E. Brundage. Hydration of $\beta''Al_2O_3$. Solid State Ionics Proceedings 9 and 10, p. 237-244.

25. F. Harback. Further experiments concerning the water takeup of fully and partially stabilized beta alumina ceramics. Solid State Ionics 9 and 10, p. 231 (1983).

26. J. Garbarczyk, W. Jakubowski and M. Wasiucionek. Effect of selected mobile ions on moisture uptake by beta alumina ceramics. Solid State Ionics 9 and 10, p. 249 (1983).

27. S. N. Heavens. Surface layers in polycrystalline sodium βAl_2O_3. Jrnl. of Mat. Sci. 17 (1982), 965-969.

28. EPRI Rept. E.M, 494, Substructure and properties of sodium beta alumina electrolytes. 1977.

29. B. Dunn. Effect of air exposure on the resistivity of sodium beta and beta" alumina. Jrnl. Amer. 64, No. 3, March 1981, p. 125.

30. B. Dunn, R. M. Ostrom, R. Servers and G. C. Farrington. Divalent cation-conductivity in beta" alumina. Solid State Ionics (1981), p. 203-204.

31. B. Dunn and G. C. Farrington. Fast divalent ion conduction in Ba^{2+}, Cd^{2+}, Sr^{2+}, Beta" alumina. Mat. Res. Bull Vol. 15, p. 1773-1777, 1980.

32. E. E. Hellstrom and R. E. Brenner. Preparation and properties of polycrystalline divalentcation $\beta''Al_2O_3$. Solid State Ionics II (1983), 125-132.

33. A. Pechenih, M. A Ratner and D. H. Whitmore. Mixed divalent and monovalent ionic conductivity in $\beta''Al_2O_3$ of a Monte Carlo study. Solid State Ionics (1983), p. 287.

34. J. O. Thomas, M. Alden and G. J. Farrington. The relationship between structure and ionic conductivity in divalent $\beta''Al_2O_3$. Solid State Ionics (1983), p. 301.

35. M. Alden, J. O. Thomas and G. Farrington. Structure of Ba^{2+} and Ca^{2+} $\beta''Al_2O_3$. Solid State Ionics 5 (1981), 205-206.

36. I. Yasui and R. H. Doremus. Effect of calcium, otassium and iron ions on degradation of $\beta''Al_2O_3$. Jrnl. Electrochem. Soc. July 1978, p. 1007.

37. Y. Lazennec, C. Lasne, Margotin and J. Fally. Factors influencing the life time of pure beta alumina electrolyte. Jrnl. Electrochem. Soc. June 1975, vol. 122, p. 734.

38. Breiter and B. Dunn. Time dependence of the asymmetric resistance of polycrystalline $\beta''Al_2O_3$. Electrochem. Acta Vol. 26, No. 9, p. 1247, 1981.

39. M. W. Breiter, B. Dunn and R. W. Powers. Assymetric behavior of beta" alumina. Electrochem. Acta Vol. 25, p. 613 (1980).

40. D. S. Demott. Resistance rise in sodium--sulfur cells. J. Electrochem. Soc. p. 2312, vol. 127 (1980).

41. G. Lehnert and B. Hartmann. Investigation for the elimination of the asymmetric resistance behavior of sodium/sulfur cells. Extende d abstract for 162th Tall meeting, Detroit.

42. Electrochemistry of solid electrolytes, 1978. Izdatel'stvo "khimiya" Moscow.

This report was done with support from the Department of Energy. Any conclusions or opinions expressed in this report represent solely those of the author(s) and not necessarily those of The Regents of the University of California, the Lawrence Berkeley Laboratory or the Department of Energy.

Reference to a company or product name does not imply approval or recommendation of the product by the University of California or the U.S. Department of Energy to the exclusion of others that may be suitable.

TECHNICAL INFORMATION DEPARTMENT
LAWRENCE BERKELEY LABORATORY
UNIVERSITY OF CALIFORNIA
BERKELEY, CALIFORNIA 94720